OPTIMAL DESIGN OF LARGE RACEWAY CULTURE SYSTEMS FOR MICROALGAE

MISS KAWISRA SOMPECH

A SPECIAL RESEARCH PROJECT SUBMITTED IN PARTIAL FULFILLMENT
OF THE REQUIREMENTS FOR
THE DEGREE OF MASTER OF ENGINEERING (CHEMICAL ENGINEERING)
FACULTY OF ENGINEERING
KING MONGKUT'S UNIVERSITY OF TECHNOLOGY THONBURI
2011

Optimal Design of Large Raceway Culture Systems for Microalgae

Miss Kawisra Sompech B.Sc. (Industrial Chemistry)

A Special Research Project Submitted in Partial Fulfillment
of the Requirements for
The Degree of Master of Engineering (Chemical Engineering)
Faculty of Engineering
King Mongkut's University of Technology Thonburi
2011

Special Research Project Committee

..... (Asst. Prof. Asawin Meechai, Ph.D.)	Chairman of Special Research Project Committee
..... (Assoc. Prof. Thongchai Srinophakun, Ph.D.)	Member and Special Research Project Advisor
..... (Asst. Prof. Jindarat Pimsamarn, Ph.D.)	Member of Special Research Project Committee

Special Research Project Title	Optimal Design of Large Raceway Culture Systems for Microalgae
Special Research Project Credits	6
Candidate	Miss Kawisra Sompech
Special Research Project Advisor	Assoc. Prof. Dr. Thongchai Srinophakun
Program	Master of Engineering
Field of Study	Chemical Engineering
Department	Chemical Engineering
Faculty	Engineering
B.E.	2554

Abstract

Raceway pond is one type of open-pond systems which has become the most popular for outdoor algal production. However, the cost of pond operation depends not only on the mixing system but also the raceway pond design. The dead zone is the sensible area causing algae cell to settle and die. This research focuses on the design of a large raceway pond concerning the energy consumption and the size of dead spot area. The two-phase model (solid-liquid) is studied by computational fluid dynamics in order to visualize the flow pattern of seawater and to allocate the position of dead spot in the returned bends of raceway. The proposed design models are the central baffle model and flow deflector baffles. These two models are compared with the standard model of raceway. This studied raceway pond has a total surface area of 0.5 hectare (5000 m^2) with fixed 8 meters width and 0.3 meters height. This system applies physical properties of *Spirulina platensis* at 20°C of seawater temperature. The simulation results show that the rotational speed of a paddle wheel directly affects the seawaterflow velocity. All of model in this research are then compared at the same velocity. As a result, the central baffle model can eliminate the vortex flow which regularly occurs behind the central baffle but still has the dead zone at the outer bend. The deflector baffle in series are studied in a number of baffles added (three is maximum). In addition, the three deflector baffles provide the optimum operating condition in terms of the energy consumption and the dead zone area reduction. Therefore, this model is proposed as the main concept to develop a new configuration. With the new model, the comparison to the standard configuration at the average velocity of 0.14 $m \cdot s^{-1}$, showed that this model can reduce the energy requirement by about 18.4% and also eliminate all of the dead area at bends.

Keywords : Raceway pond design / Flow deflector baffle / Central baffle / Algae cultivation

หัวข้อโครงการศึกษาวิจัย	การออกแบบที่เหมาะสมสำหรับระบบรางน้ำเพาะปลูกสาหร่ายขนาดใหญ่
หน่วยกิต	6
ผู้เขียน	นางสาวกวิสรา สมเพชร
อาจารย์ที่ปรึกษา	รศ.ดร.ธงไชย ศรีนพคุณ
หลักสูตร	วิศวกรรมศาสตรมหาบัณฑิต
สาขาวิชา	วิศวกรรมเคมี
ภาควิชา	วิศวกรรมเคมี
คณะ	วิศวกรรมศาสตร์
พ.ศ.	2554

บทคัดย่อ

บ่อรางน้ำเป็นระบบที่ถูกนำมาใช้มากที่สุดสำหรับการเพาะปลูกสาหร่ายภายนอกอาคาร อย่างไรก็ตาม ต้นทุนในการดำเนินงานที่ใส่เข้าไปในระบบนั้น ขึ้นอยู่กับระบบการผสมรวมทั้งการออกแบบรูปร่างของบ่อรางน้ำ นอกจากนี้บริเวณที่มีความเร็วต่ำเป็นบริเวณที่มีความไวต่อการตกตะกอนของสาหร่ายและส่งผลให้สาหร่ายตายในที่สุด งานวิจัยนี้ได้ศึกษาการออกแบบบ่อรางน้ำขนาดใหญ่ที่ส่งผลต่อการบริโภคพลังงานในระบบและส่งผลต่อขนาดของบริเวณที่มีความเร็วต่ำ โดยสร้างแบบจำลองการไหลแบบสองสถานะ (ของแข็ง-ของเหลว) โดยใช้วิธีวิเคราะห์พลศาสตร์ของไหลโดยคอมพิวเตอร์มาแสดงรูปแบบการไหลของน้ำทะเลและตำแหน่งของบริเวณที่มีความเร็วต่ำโดยเฉพาะอย่างยิ่งในบริเวณที่มีการเลี้ยวกลับของบ่อรางน้ำ การออกแบบแบบจำลองที่ถูกนำมาศึกษาในงานวิจัยนี้ได้แก่ แบบจำลองผนังกั้นกลาง และแบบจำลองของชุดแผ่นกั้นที่ปลายบ่อสองด้าน แบบจำลองสองแบบนี้จะถูกนำไปเปรียบเทียบกับแบบจำลองทั่วไปของบ่อรางน้ำ ซึ่งงานวิจัยนี้กำหนดให้ขนาดพื้นที่ของบ่อรางน้ำมีขนาดพื้นผิวเท่ากับ 0.5 เฮคเตอร์ (5,000 ตารางเมตร) โดยยึดความกว้างของบ่อที่ 8 เมตร และความสูงที่ 0.3 เมตร งานวิจัยนี้ได้นำคุณสมบัติทางกายภาพของสาหร่ายเกลียวทองมาใช้ในการวิเคราะห์ และกำหนดอุณหภูมิเพาะปลูกที่ 20 องศาเซลเซียสน้ำทะเล ผลการศึกษาแสดงให้เห็นว่าความเร็วรอบของใบพัดส่งผลกระทบโดยตรงต่อความเร็วในการไหลของน้ำทะเลในทุกกรณี อย่างไรก็ดีแบบจำลองทุกรูปแบบในงานวิจัยนี้จะถูกเปรียบเทียบที่ความเร็วเฉลี่ยของน้ำทะเลที่ค่าเท่ากัน ผลการศึกษาพบว่าแบบจำลองผนังกั้นกลางสามารถกำจัดการไหลปั่นป่วนที่มักเกิดขึ้นที่ด้านหลังของผนังกั้นกลางได้ แต่จะยังคงพบบริเวณที่มีความเร็วต่ำในส่วนโค้งนอกของบริเวณที่มีการเลี้ยว ในขณะที่แบบจำลองแผ่นกั้นที่ปลายบ่อสองด้านได้ถูกศึกษาในเรื่อง

ของจำนวนแผ่นกั้นที่ใส่เข้าระบบ (มากที่สุดสามแผ่น) และพบว่าการใช้ชุดแผ่นกั้นสามแผ่นให้ผลดีที่สุดในเรื่องของการใช้พลังงานและการลดบริเวณที่มีคามเร็วต่ำ ดังนั้นแบบจำลองชุดแผ่นกั้นสามแผ่นนี้จึงถูกเสนอเป็นแนวความคิดหลักเพื่อพัฒนาเป็นแบบจำลองใหม่ สำหรับแบบจำลองใหม่เมื่อนำไปเปรียบเทียบกับรูปแบบทั่วไปของบ่อรางน้ำที่ความเร็วเฉลี่ยของน้ำเท่ากับ 0.14 เมตรต่อวินาที พบว่าแบบจำลองปรับแต่งสามารถลดการใช้พลังงานลงได้ราว 18.4 เปอร์เซ็นต์ ในขณะเดียวกันก็สามารถกำจัดบริเวณที่มีความเร็วต่ำที่บริเวณเลี้ยวโค้งได้ทั้งหมด

คำสำคัญ : การออกแบบบ่อรางน้ำ / แผ่นกั้นปลายบ่อ / ผนังกั้นกลาง / การเพาะปลูกสาหร่าย

ACKNOWLEDGEMENTS

This project would not have been completed without direct and indirect assistance from many people. Foremost, the author would like to express his gratitude to the advisor of this project, Assoc. Prof. Thongchai Srinophakun for all technical support, valuable guidance and encouragement. The author also appreciates the supervisor, Prof. Yusuf Chisti, professor of Biochemical Engineering in the School of Engineering at Massey University, for his valuable suggestion and comments during oversea study. In addition, the author would like to appreciate to Asst. Prof. Dr. Asawin Meechai and Asst. Prof. Dr. Jindarat Pimsamarn, project committees, for attention to this research project and their useful advices.

Moreover, the author would like to thank Mr. Nattapong Tarapoom and Mr. Thanasan Tangchaksuwan for their suggestions and their computer time bestowing. The author would like to express his gratitude to WATA server of Kasetsart University for software supporting. The author particularly express special thanks to the staff of Chemical Engineering Practice School (ChEPS), Mrs. Chadaporn Dammunee, who helped the author with communication and any important information used to finish the master degree. Lastly, this project would not have been completed without lots of support from the author's family and friends.

CONTENTS

LIST OF TABLES

LIST OF FIGURES

NOMENCLATURES

A_P	=	Area of the paddle in a plane perpendicular to the direction of the motion
CFD	=	Computational fluid dynamics
C_D	=	Drag coefficient for flat paddles
d	=	Depth of liquid
Δd	=	Change in water depth
e	=	Efficiency of a paddle wheel
ε	=	Dissipation
ε_α	=	Phase volume fraction
F_P	=	Drag force on a paddle wheel
ha	=	Hectares
k	=	Turbulence kinetic energy
L	=	Channel length
M_α	=	Interfacial forces acting on phase due to the presence of other phases
m_{object}	=	The true (vacuum) mass of the object
μ	=	Viscosity
n	=	Manning's roughness
N_p	=	Number of phase
P	=	The power
P_P	=	The power required for mixing by the paddle wheel
ρ	=	Density
ρ_α	=	Phase density
ρ_{fluid}	=	Average densities of the object
ρ_{object}	=	Average densities of the object
Q	=	Quantity of water in motion
R_h	=	Mean hydraulic radius or depth for wide channels
$Re_{channel}$	=	Renold’s number of open channel
S	=	Rate of head loss per unit length
$S_{M\alpha}$	=	Momentum sources due to external forces
u_α	=	Phase velocity
v	=	Flow velocity
v_P	=	Velocity of paddle relative to water
W	=	Specific weight of culture medium
w_c	=	Channel width
$\Gamma_{\alpha\beta}$	=	Mass flow rate per unit volume from phase α to β
$\frac{\partial \rho}{\partial t}$	=	Rate of increase of mass per unit volume

$\nabla \cdot \rho v$	=	Net rate of mass addition per unit volume by convection

CHAPTER 1 INTRODUCTION

1.1 Background

Following the energy crisis and the accumulation of greenhouse effect gases in the atmosphere, there are diverse schemes that studied to handle these problems. The utilization of microalgae as a biomass fuel and carbon dioxide conversion technologies could potentially contribute to solution of these global problems in the future. Microalgae can be cultivated in the large outdoor ponds by consuming the resources of carbon dioxide gas, sunlight, culture medium and other necessary nutrients. The productivity rates of microalgae are higher than most of other plants [1, 2]. These rates indicate that magnitude microalgae productivity can be obtained in outdoor culture ponds. Commercial-scale culture of microalgae generally requires culture volumes of 10,000 to greater than 1,000,000 liters [3]. Open-pond or channel-type systems, such as raceways have become the most popular for outdoor algal production because they are cheaper to build and operate than closed photobioreactors. However, the cost of pond operation and the energy input efficiency depend on the mixing system and the raceway pond design.

Considering to the raceway pond, the design aids to minimize the amplitude of eddy formation, and to eliminate stagnant zone in order to avoid solid deposition occurring at the back side of the center wall. The mixing system can promote many operating conditions including the prevention of cell settling to ensure the equal light exposing, the elimination of thermal stratification, the distribution of nutrients and carbon dioxide, the removal of photosynthetically produced oxygen, and the improvement of light utilization efficiency. To ensure adequate mixing, a minimum liquid circulation velocity should be maintained at level of 0.05-0.3 $m \cdot s^{-1}$ [4]. Paddle wheel has been the most acceptable way to maintain this velocity in open raceways. Generally, the curved flow deflectors need to be considered to minimize the eddy formation and the velocities that can keep away the solids deposition on the back side of the center wall and baffles. Moreover, the design of the central baffle also received an interesting in existing plant to overcome the dead zone area.

In this study, Computational Fluid Dynamics (CFD) was used to predict the flow pattern. This tool is widely acceptable for engineering works for predictation of flow behavior because it is reliable, convenient and cost-effective time consumption. The CFD method including both computational and modeling features, has been demonstrated mechanistically based numerical simulations of multi-phase flows. The major objective of the work is to propose an improvement geometric design of the central baffle and flow deflector baffle in such a way that the energy required for circulation is minimized and also keep algal cells in suspension.

1.2 Objective

This research proposes the optimal raceway pond model based on flow deflector baffle and central baffle design. This model gives the sufficient flow to suspend the algal cells and can approach the energy efficiency.

1.3 Scopes of work

1. Use CFD program (ANSYS 13.0) to simulate flow behavior inside the raceway to predict the velocity profile and the energy consumption and concern the algae growth factor only the mixing condition

2. Propose the modifications design of the large raceway culture system which concentrate on geometric design to achieve the optimum results

3. Perform the simulation conducted by Massey University or assessment of the work in the literature (such as the raceway size and assumptions which were shown in the methodology chapter)

CHAPTER 2 THEORY AND LITERATURE REVIEWS

2.1 Cultivation of microalgae in outdoor ponds

Open pond or raceway pond is the oldest and simplest system for mass cultivation of microalgae. This cultivation method currently has become the best alternative for commercial-scale culture when compared with other systems. The reason comes from its high productivity over 1,000 gallons per acre annually and its production costs at approximately 20 cents per pound cheaper than closed photobioreactor [5]. These will result in low production costs for algae biomass. There are various algae species which have been grown successfully in outdoor ponds such as *Spirulina platensis* [6], *Dunaliella salina, Haematococcus pluvialis, and Nannochloropsis*. This chapter describes the key features of raceway design with particular emphasis on large-scale commercial culture and reviews the literature related to microalgae cultivation.

Because of confidential contracts, there are a few literature reviews on actual commercial algae cultivation. Nevertheless, the outdoor culture process description of each species can be followed to these reports, *Spirulina* [7, 8, 9], *Dunaliella* [10, 11, 12], *Chlorella* [13, 14, 15] and *Haematococcus* [16, 17]. *Oswald* [18] presented the using microalgae for wastewater treatment. Furthermore, cyanobacteria production for biofertilizers is reviewed by *Kaushik* [19].

2.2 Types of open ponds

Algae can be grown in sunny areas using open ponds. All types of interesting large-scale outdoor pond for microalgae cultivation have been generated and basically categorized into rectangular pond or raceway pond, circular pond, large shallow pond (extensive) and deep pond. Raceway pond and circular pond are more prevalent than the other two types. Therefore, the suitable type frequently used on a commercial scale is a raceway pond.

Circular ponds with a rotating arm which are the oldest large-scale culture are used in Taiwan for the production of *Chlorella*. These circular ponds are constructed based on similar systems used in wastewater treatment. Depth is about 30 cm. The Pond areas are limited to about 10,000 m^2 because of mixing condition of rotating arm in larger ponds. This pond type is shown in Figure 2.1a.

Individual raceway ponds (rectangular ponds with a paddle wheel) are usually about 20 to 30 cm deep and up to 1 ha in area. Flow mixing is generated by a paddle wheel that can circulate water with nutrients and microalgae (Figure 2.1b). For the raceway with added baffles, the baffles in the channel has obligation to guide the flow around the bends in order to minimize space. This open pond type is the most widely used for the production of *Spirulina, D. salina*, and *Haematococcus* [4]. However, this system is easily contaminated. Only a few species of microalgae can be grown in these open systems with their environmental requirement (e.g. high salinity for *Dunaliella salina* and high alkalinity with *Spirulina platensis*.).

Commercial-scale pond is ranged in total surface area from about 0.5 to 1.0 ha for a raceway or central pivot ponds and up to 200 ha or more for the extensive ponds used in the culture of *D. salina* [4].

Figure 2.1 (a) Center-pivot pond used for the cultivation of Chlorella in Taiwan
(b) Raceway ponds used for the culture of Spirulina by Microbio Inc. at Calipatria, California [4].

2.3 Ponds mixing

Mixing is necessary to prevent the settling of cells, to avoid thermal stratification, to distribute nutrients and break down diffusion gradients at the cell surface, to remove photosynthetically generated oxygen, and to ensure that all the cells experience alternating

periods of light and darkness. Furthermore, many experiences have shown that the ponds which supplied sufficient mixing achieve higher productivities and more stable cultures [3, 20, 21, 22]. The maximum concentration of algae production in unmixed pond is about 0.1 $g \cdot L^{-1}$ dry weight, compared with the algae grown in adequate mixing raceway, which achieve dry weight up to 1.0 $g \cdot L^{-1}$.

In a large raceway culture, a low velocity is difficult to maintain algae cells in suspension because of frictional losses in the raceway and losses due to irregularities of the pond lining material. Flow velocities of 10 to 30 $cm \cdot s^{-1}$ are recommended in practice. Higher turbulence enhances more growth, and then extra device used to mix and circulate the flow should be installed in the raceway. However, the higher flow rate needs the higher energy. This extra turbulence-generator leads to increase the operating costs [18].

Some form of mixing is required to maintain cells in suspension, to prevent thermal stratification, and to disperse nutrients. The most widely used formula for open channel flow is the Manning's equation [18]:

$$v = \frac{R_h^{2/3} S^{1/2}}{n} \tag{2.1}$$

where:

	v	=	velocity, $(m \cdot s^{-1})$
	R_h	=	mean hydraulic radius, (m)
	S	=	head loss / unit length, (dimensionless)
	n	=	Manning's roughness, $(s \cdot m^{-1/3})$

R_h is the flow area (A) divided by the perimeter in contact with the water (P)

$$R_h = \frac{A}{P} = \frac{dw_c}{(w_c + 2d)} \tag{2.2}$$

where:

	w_c	=	the channel width
	d	=	the depth

For very wide and shallow channels, R_h is approximately equal to the depth (d). The rate of head loss (S) is in the channel per unit length, that is, $\Delta d \cdot L^{-1}$(dimensionless), where Δd is the change in water depth and L is the channel length; and n = Manning's friction coefficient, a measure of channel roughness. Table 2.1 gives estimated mean values for Manning's n in open channels constructed of various materials [18].

The Manning's equation can be rearranged to solve for the head loss:

$$S = \frac{v^2 n}{R_h^{4/3}} \tag{2.3}$$

and $$S = \frac{\Delta d}{L} \tag{2.4}$$

thus $$\Delta d = \frac{LV^2 n^2}{[dw/(w+2d)^{4/3}]} \tag{2.5}$$

Table 2.1 Estimated mean value for Manning's n in open channels.

Materials for channel liner	**Manning's n value**
Smooth plastic on smooth concrete	0.008
Plastic with "scrim" on smooth earth	0.010
Smooth plastic on granular earth	0.012
Smooth cement concrete	0.013
Smooth asphalt concrete	0.015
Coarse trowelled concrete, rolled asphalt	0.016
Gunnite or sprayed membranes	0.020
Compacted smooth earth	0.020
Rolled coarse gravel, coarse asphalt	0.025
Rough earth	0.030

Flow in an open channel can be either laminar or turbulent depending upon the Reynolds number, Re.

Reynolds Number calculation for open channel [23]:

$$Re_{channel} = \frac{vR_h}{\mu} \tag{2.6}$$

And the limits for each type of flow are

$$\text{Laminar}: \ Re_{channel} < 500$$
$$\text{Turbulent}: \ Re_{channel} > 1000$$

In practice, the limit for turbulent flow is not so well defined in channel as it is in pipes. Therefore, the value of 2000 is often taken as the threshold for turbulent flow. However, the data from operating experiment indicated that the flow rate in a raceway pond should be in range of 0.05-0.3 $m \cdot s^{-1}$ [4]. This velocity range can achieve the high turbulence as shown in appendix A.

The mixing power requirement can be calculated from the head losses, the channel dimensions, and the speed by following equation (2.7).

$$P = QW\Delta d / 102e \quad (2.7)$$

where: P = the power (kW)
Q = the quantity of water in motion ($m^3 \cdot s^{-1}$)
W = the specific weight of culture medium ($kg \cdot m^{-3}$)
e = the efficiency of a paddle wheel; 102 is the conversion factor required to convert $m \cdot kg \cdot s^{-1}$ to kW

For a channel of width w_c and depth d, the quantity of flow Q is given by

$$Q = w_c dv \quad (2.8)$$

The specific weight of culture medium is depended on the medium temperature and the sort of medium. An average value of efficiency is about 0.17 for paddle wheels operating over a flat bottom. These data can be used for ponds without a sump as a general indicator. However, paddle wheels with sumps are more efficient [24].

Paddle wheel is generally used as turbulence-generator device for a raceway pond. It is easy to maintain and is the high efficient tool for mixing the algal culture. The design of a paddle wheel also affects the flow rate and the energy requirements (as can see in later details).

2.4 Paddle wheel

Paddle wheels are the high efficient tools for mixing the algal culture as the following reasons: 1) They are well matched to the pumping requirements of high-rate ponds in high volume and low head devices (i.e. high specific speed); 2) Their gentle mixing action minimizes the damage of colonial or flocculated algae, to improve the harvest ability; 3) They are mechanically simple, requiring a minimum of maintenance; 4) Their drive train can easily be designed to accommodate a wide range of speeds (high turn-down ratio) without drastic changes in efficiency; 5) They do not require an intake sump, but simply a shallow depression for maximum efficiency [24].

Paddle wheel design of *Dodd* [25] is described here to review its standard size. This paddle wheel locates in a depression or invagination (sump) on the pond bottom. A clearance between the blades and the bottom is maintained by this sump, hence the backflow can be reduced. At least one blade is needed to sit in the sump at all times to minimize this constant clearance value. Therefore, the minimum space of the sump can be figured from a given diameter of a paddle wheel with a particular number of blades.

The smaller the clearance between the blade and the pond floor also means the more efficient a paddle wheel. The recommended clearance on both sides and the bottom is about of 20 mm [4]. Moreover, a larger paddle wheel diameter leads a lower mean back-flow in a raceway pond but this greater diameter also means a higher construction cost. Consequently, a suitable diameter is 1,500 mm (generally used). Finally, the higher number of paddle wheel blades means the higher the paddle wheel efficiency and the less the motor

shock. In practice, a paddle wheel with more than eight blades is not suggested from the construction feasibility and does not significantly improve the paddle wheel efficiency [4].

In terms of power required for mixing by the paddle wheel (P_P), it can be found from;

$$P_P = F_P v_P \tag{2.9}$$

where: F_P = the drag force on a paddle wheel, (N)

v_P = the velocity of paddle relative to water, ($m \cdot s^{-1}$)

And the drag force can be estimated from;

$$F_P = \frac{C_D A_P v_P^2}{2} \tag{2.10}$$

where: C_D = the drag coefficient for flat paddles

A_P = the area of the paddle in a plane perpendicular to the direction of the motion, (m^2)

Hence, the power required for mixing by the paddle wheel can be found from combining Equations (2.9) and (2.10).

$$P_P = \frac{C_D A_P v_P^3}{2} \tag{2.11}$$

2.5 Flow deflector

The structure and operation of flow deflector have been described in *Shimamatsu and Tominaga* [26] and *Shimamatsu* [27]. These flow deflectors are turning vanes in the pond with right-angled corners. Turning vanes are widely used in analogous fluid system (i.e. air ducts). They consist of closely spaced turning vanes placed along the diagonals from the center wall to the corners of the pond (see Figure 2.2a). If closely spaced (i.e. at intervals equal to the pond depth) and the vanes are quite efficient, and virtually eliminate problems of eddy formation and solids deposition. These rectifiers are most easily installed after the lining and simply sit on the plastic surface at the corners of the pond.

An alternative adjustment to turning vanes rectifiers are curved deflectors which consists of an eccentrically placed curved walls and baffles at the end of the pond furthest away from the paddle wheel [25]. The curved flow deflectors aid in minimizing the extent of eddy formation and the stagnant zone downstream of the bend (Figure 2.2b). This creates a curved zone of accelerating flow, followed by a flow expansion zone after the directional change has been made. The rate of constriction of the curved zone is sufficient to reduce eddy formation or velocities below that causing solids deposition on the back side of the center wall and baffles. The channel constriction technique is also used at the other end of the pond, which allows access to a paddle wheel [24].

The quantity of material required for both curved deflectors and vanes is about the same, but the latter requires more elaborate support and would be more expensive to install.

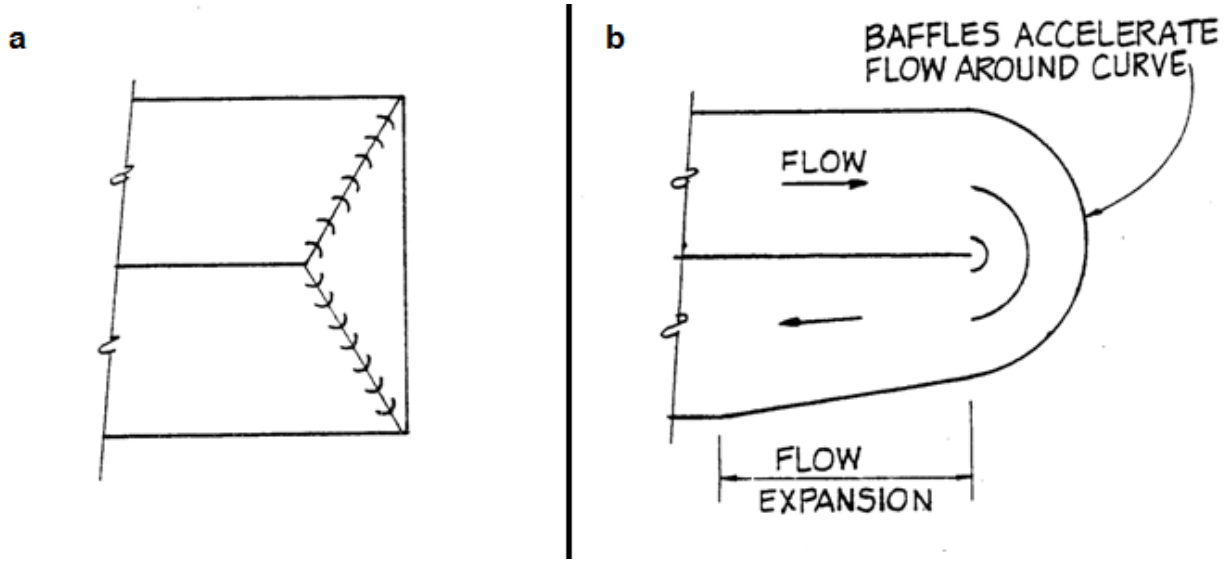

Figure 2.2 Existing flow deflector option (a) Square end walls and turning vanes and (b) Curved end walls and flow deflector [24].

2.6 Computational fluid dynamics

Computational Fluid Dynamics (CFD) is a computer-base tool for predicting the performance of the system concerning the mass transfer, heat transfer, chemical reaction, fluid flow and related phenomena by solving the mathematical equations. This tool incorporates the solution of the fundamental equations of fluid flow, the Navier-Strokes equations and other allied equation [28]. The results of CFD models are significant engineering data used in concept of new designs, modified model and developed product.

2.6.1 CFD Procedures

The basic procedures of all CFD programs are similarly and generally divided into 4 steps as follow:

- Defining the geometry and creating the mesh of control volume
- Selecting the physical models
- Simulating the model by solving equations
- Analyzing and visualizing the results in the post-processor

2.6.1.1 Defining the geometry and creating the mesh of control volume

This is the first step in building and analyzing model. Mesh is created after the body of geometry was produced. Then, this mesh is used as an input file in preprocessing step. Users can mesh the interest geometry region by geometry/mesh creation tools. The accuracy of a CFD solution is governed by the number of elements and nodes which were created in mesh creation tools. Generally, the larger the number of elements is, the better the solution accuracy is, and the longer the computational time is.

2.6.1.2 Selecting the physical models

The user's activities at the pre-processing stage involve the selection of the physical and chemical phenomena, and the specification of appropriate boundary conditions. The solution of flow problem (velocity, pressure, temperature, etc.) is defined at modes inside each cell.

2.6.1.3 Solving CFD problem

After the preprocessing step, all flow problems are solved by using the suitable numerical methods. There are three important methods of numerical solution techniques: finite difference, finite element and finite volume. The solving processes are shown as below:

- The partial differential equations are integrated over all the cells in the region of interest.
- Integral equations are converted to a system of algebraic equations by generating a set of approximations for the terms in the integral equations.
- The algebraic equations are solved iteratively.

2.6.1.4 Analyzing and visualizing the results in the post-processor

This is the final step in CFD analysis, and it involves the organization and interpretation of the predicted flow data and the production of CFD images and animations. The post-processing is used to display the results as with the preprocessing. Typical picture obtained with the post-processing might contain a section of the mesh together with vector plots of velocity field.

2.6.2 Mathematic model for raceway pond

Water flow and algal cell distribution was determined with the CFD code. This code uses the finite element method for the discrimination of the Navier-Stokes equations. Since the raceway pond configuration is very large and flat, this work had to generate only 2 phases of fluid (seawater) and solid (algae) that can converse easier than using 3 phases and achieved a good result of flow pattern and solid settling in the raceway. The mathematical model is based on liquid-solid multiphase flow model. The inhomogeneous model in

Eulerian-Eulerian multiphase flow that applied for the two-phase liquid-solid flow is used in this work. That means the laws of conservation of mass and momentum are satisfied by each phase individually. Standard governing equations (mass and momentum conservation equations) were considered in the present work.

Under usual operating condition, turbulent flow (mixing) is required to suspend algae cell and enhance growth. Turbulent stresses are modeled using $k-\varepsilon$ model. This model has been implemented in most general purpose CFD codes and is considered the industry standard model. It has proven to be stable and numerically robust and has a well established regime of predictive capability. For general purpose simulations, the $k-\varepsilon$ model offers a good compromise in terms of accuracy and robustness. The following dependent variables are solved for each phase separately.

2.6.2.1 Continuity equation

The continuity equation is developed by a mass balance over a control volume element, fixed in space, through which a fluid flowing. This equation describes the time rate of change of the fluid density at a fixed point in space. This equation can be written using vector notation as follow:

$$\frac{\partial \rho}{\partial t} = -(\nabla \cdot \rho v) \tag{2.12}$$

where: $\frac{\partial \rho}{\partial t}$ = Rate of increase of mass per unit volume

$\nabla \cdot \rho v$ = Net rate of mass addition per unit volume by convection

This research focuses on the behavior of two-phase flow; a liquid and a solid phase. The flow behavior of each phase can be described in following context. The fundamental form of the equation for multiphase flows with N_p phases means for phase α. It can be described as follows:

$$\frac{\partial_\alpha \rho_\alpha}{\partial t} + \nabla \cdot \left(\varepsilon_\alpha \rho_\alpha u_\alpha\right) = \sum_{\beta=1}^{N_p} \Gamma_{\alpha\beta} + \mathrm{S}_{\mathrm{M}\alpha} \tag{2.13}$$

where: ε_α = Phase volume fraction

ρ_α = Phase density

u_α = Phase velocity

$\mathrm{S}_{\mathrm{M}\alpha}$ = Momentum sources due to external forces

$\Gamma_{\alpha\beta}$ = Mass flow rate per unit volume from phase α to β

N_p = Number of phase

The terms on the left-hand side of this equation describe the internal change of mass over time and the convective flux crossing the boundaries of the volume. On the right-hand side, the first term describes mass transfer from phase α to β and while the second term includes additional source terms. In any terms of this equation consist of ε_α variable. This ε_α is the volume fraction of phase α, which needs to satisfy the relation

$$\sum_{\alpha=1}^{N_p} \varepsilon_\alpha = 1 \qquad (2.14)$$

For this work, the fluid model consists of two phases. In the case of a two-phase flow with one liquid and one solid phase, the phase volume fraction requirement reduces to $\varepsilon_l + \varepsilon_s = 1$.

where: ε_l = liquid volume fraction

ε_s = solid volume fraction

2.6.2.2 Momentum equation

Momentum equation is related to the Newton's second law of motion. This equation is used to explain the transfer of the interested fluid in a control volume. The momentum equation for multiphase flows is described by Navier-Strokes equation expanded by the phase volume fraction.

$$\frac{\partial(\varepsilon_\alpha \rho_\alpha u_\alpha)}{\partial t} + \nabla \cdot (\varepsilon_\alpha (\rho_\alpha u_\alpha \otimes u_\alpha)) = -\varepsilon_\alpha \nabla \rho_\alpha + \nabla \cdot \left(\varepsilon_\alpha \mu_\alpha (\nabla u_\alpha + (\nabla u_\alpha)^T) \right) + \sum_{\beta=1}^{N_p} (\Gamma^+_{\alpha\beta} u_\beta + \Gamma^+_{\alpha\beta} u_\alpha) + S_{M\alpha} + M_\alpha \qquad (2.15)$$

where: M_α = Interfacial forces acting on phase due to the presence of other phases

The terms on the right-hand side of this equation describe all forces acting on the phase α fluid element in the control volume. There are the overall pressure gradient, the viscous stresses, the momentum sources due to external forces and interphase momentum forces.

2.6.2.3 Buoyancy

For buoyancy calculation, it is familiar with buoyancy in single-phase flow. In addition to the buoyancy forces that can exist in single-phase flows, the difference in density between phases produces a buoyancy force in multiphase flows. Buoyancy acts against the force of gravity and makes objects seem lighter with respect to gravity. To represent this effect, it is

common to define a buoyancy mass (m_b) that represents the effective mass of the object with respect to gravity as follow [29]:

$$m_b = m_{object} \cdot (1 - \frac{\rho_{fluid}}{\rho_{object}}) \quad (2.16)$$

where: m_{object} = The true (vacuum) mass of the object

ρ_{object} = The average densities of the object

ρ_{fluid} = The average densities of the object

Thus, if the two densities are equal, $\rho_{object} = \rho_{fluid}$, the object appears to be weightless. If the fluid density is greater than the average density of the object, the object floats; if less, the object sinks.

2.6.2.4 Turbulence Model

In fluid dynamics, turbulence flow includes low momentum diffusion, high momentum convection and rapid variation of pressure and velocity in space and time. It is a complex process, mainly because it is in three dimensional, unsteady and consist of many scales. Turbulence occurs when the inertia forces in the fluid become significant compared to viscous force, and is characterized by high Reynold's number. In general system, turbulence flow requires the high input energy. However, for applications such as mixing ponds, turbulence flow is essential for good in mixing. Equations for single-phase turbulence model were used in the present work. A $k-\varepsilon$ model and dispersed phase zero model are respectively applied to the continuous fluid and dispersed solid phase in order to model the turbulence. For this inhomogeneous flow, it is possible to solve a single turbulence field in a similar way to homogeneous model. The well-known single phase standard $k-\varepsilon$ turbulence model is applied to turbulence phenomena in the continuous phase of the liquid-solid flow [30].

CHAPTER 3 METHODOLOGY

This work considers the pattern of fluid flow at the bends of raceway pond and aims to propose the improvement geometric design to obtain more energy efficient in the raceway and to achieve the sufficient flow velocity to suspend the algal cells which provide the minimum energy input. The flow system is calculated and analyzed by simulation. The procedures are shown in Figure 3.1.

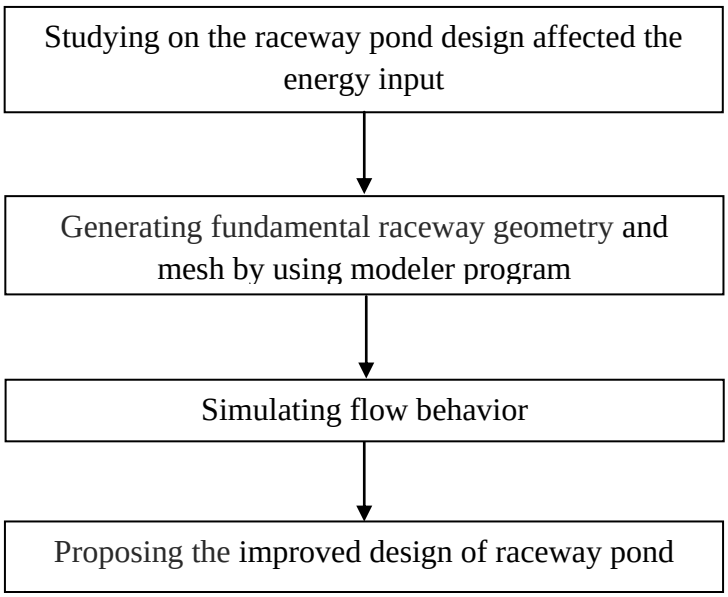

Figure 3.1 Methodology.

3.1 Studying the raceway pond design affected the energy input

The general details of open pond design and other constraints were studied by collecting data from hand books and journals. The design of raceway pond must meet numerous basic criteria (e.g., construction and maintenance costs should be low while providing the optimal energy consumption and light environment for algae). However, this work only focuses on the pond design which related to the energy consumption. Different design obtains different velocity profile, which means the new configuration can obtain more energy efficient. In the case that commercial paddle wheel was used to generate the waterflow, this study had to keep on the designs which have a direct impact on the energy input such as the flow rectifier and the central baffle.

3.2Fundamental raceway geometry and mesh generation

The general raceway pond geometry was then created based on existing commercial width scale. This configuration was modeled for a total surface area of 0.5 ha (5000 m^2) with 8 m width fixed. The geometry of the raceway pond was created using 3D software tool. In the simulation part, the volume occupied by the fluid has to be divided into many grids and calculate it in each grid about the fluid phenomena. This step is namely called "meshing". The meshing should be adjusted to high resolution and generated using infrastructure grid. The general configurations of a raceway and a paddle wheel are shown in Figures 3.2 and 3.3.

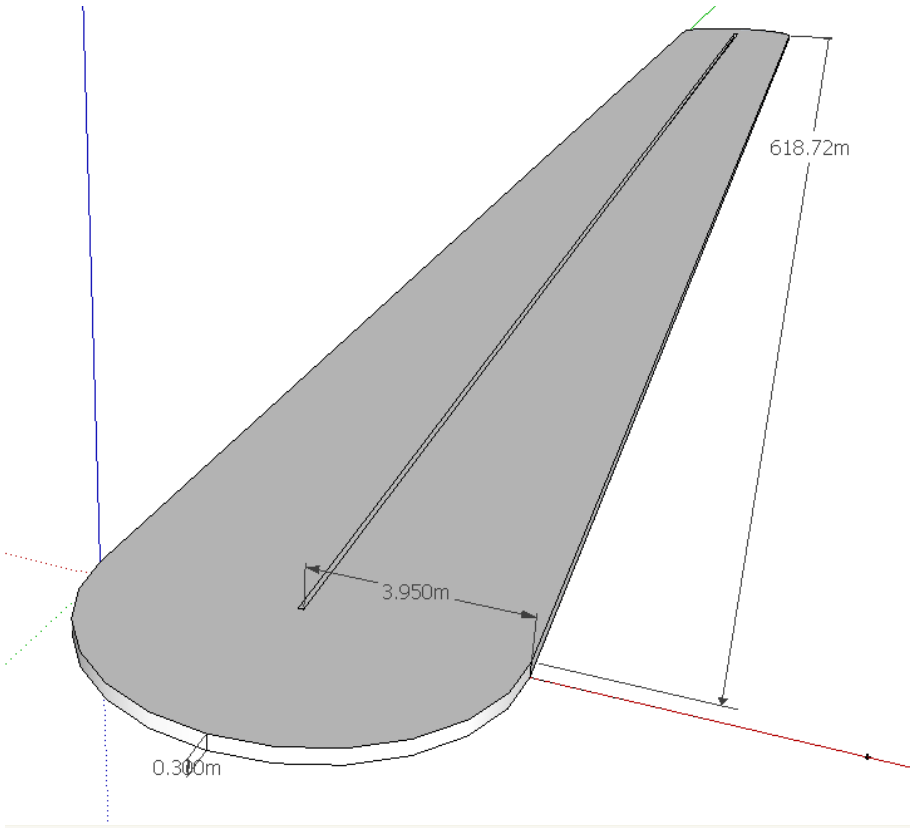

Figure 3.2 General configuration of raceway.

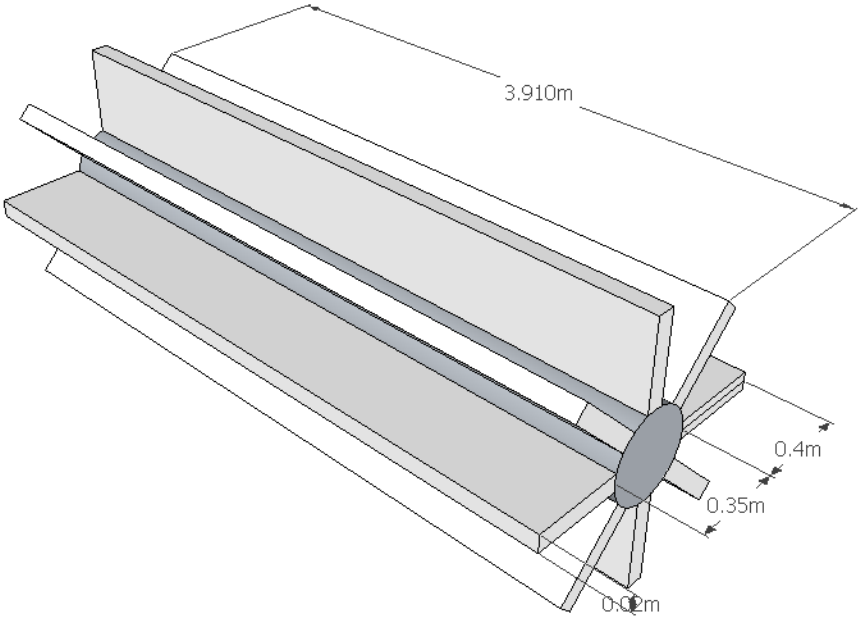

Figure 3.3 General configuration of a paddle wheel.

After mesh was produced, the meshing quality can be checked by using meshing program before input to pre-processor unit. Tetrahedral method was applied for a raceway pond domain while auto volume was applied for the paddle wheel domain (hexahedral method is proper to the rectangular paddle wheel blade shape). Figure 3.4 shows the mesh of raceway geometry with mesh's quality greater than 0.2 while Figure 3.5 shows the paddle wheel mesh which used for every raceway configuration.

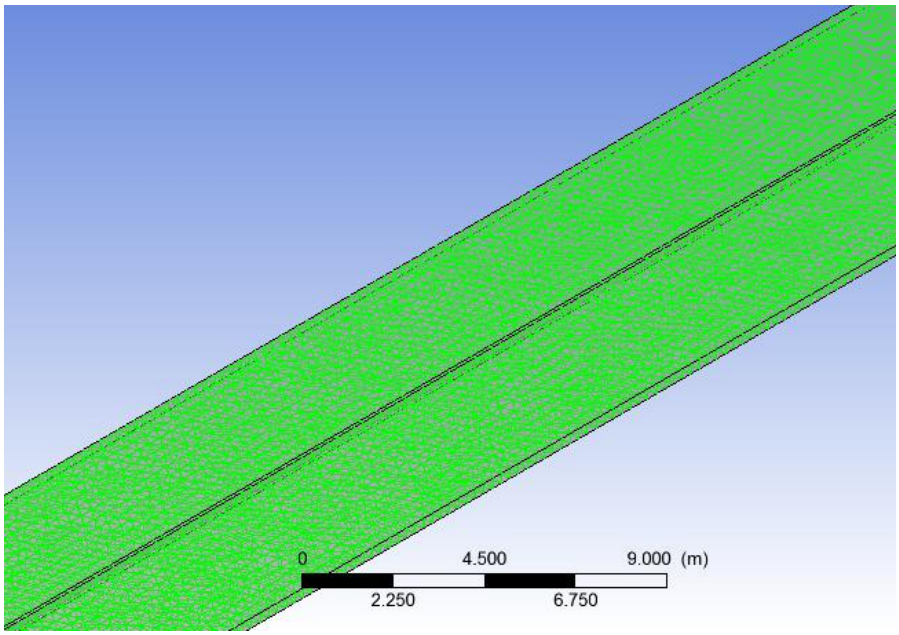

Figure 3.4 Mesh of raceway pond.

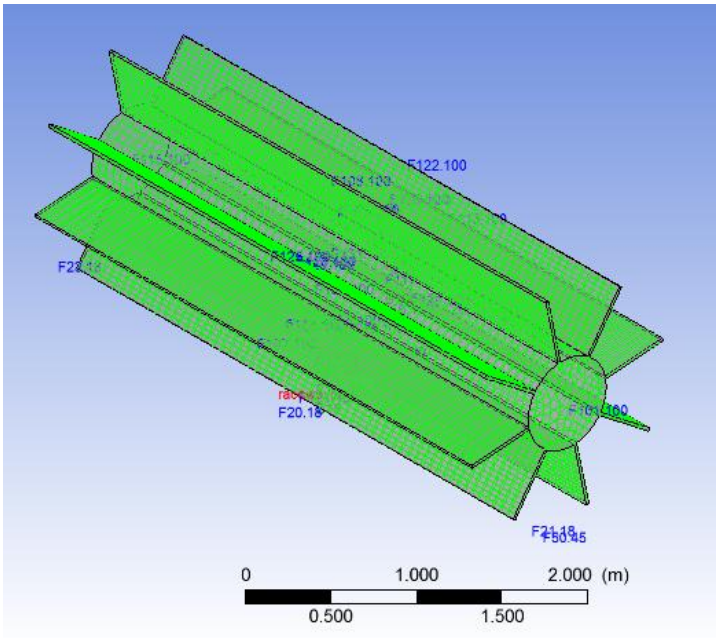

Figure 3.5 Mesh of a paddle wheel.

3.3 Simulating flow behavior

In this study, all of proposed raceway designs were tested using a computational fluid dynamics (CFD). This program uses finite volume method to solve fluid flow governing equations for steady state problem over a region of interest, with specified conditions on the boundary of that region. Under the general commercial operating conditions, the flow is found to be turbulent and turbulent stresses are modeled using k-ε model. The governing equations for multiphase was introduced to reduce computational time and followed by the initial condition and boundary conditions.

Since the raceway pond configuration is very large and flat, this work will scope only two phases of fluid (seawater) and solid (algae) to study flow pattern and evaluate the dead zone area in the raceway.

The designs of open raceway pond were fixed total surface size about 5,000 m^2. Because relatively even mixing by the commercial paddle wheel is no longer possible in channel width greater than 4 meters, all of pond design space should be 618.72 m long and 8 m width while depth is 0.3 m. Moreover, in order to avoid complication of location and number of paddle wheel that can disturb the velocity profile in the system, this study used only one paddle wheel and set it up at the middle of raceway path. The water flow velocity was maintained at the level of slightly greater than 0.1 $m \cdot s^{-1}$ (conducted by Massey University laboratory information) to keep turbulent mixing by varying revolution of paddle wheel. Calculation of Reynold's number (Re) was presented in appendix A. For

open channel flow, *Re* of over 2000 indicates turbulent flow thus the velocity of 0.1 $m \cdot s^{-1}$ shows highly turbulent and has good mixing.

There are 6 models which were simulated in this work. The first five model patterns based on existing commercial plant while last model was improved to reduce the dead zone area and obtain more energy conservation than the others.

The assumptions to model flow behavior in a raceway pond are as following

- The system was under steady state condition
- The system contained only seawater and algal cell, atmospheric air above water surface in flat system was negligible
- No slip wall condition and no wind friction above seawater surface
- Properties of seawater referred as the properties of seawater at constant temperature of 20 ^{o}C
- Algae was assumed to be dry solid and mass transfer between algal cell and water was negligible
- Algae cell had a spherical shape and constant diameter (Ø = 47.7 micron)
- Only one paddle wheel was applied to generate water flow in a raceway pond
- Heat transfer of the fluid model was neglected

Materials properties definition

A maximum dry cell concentration of 0.5 to 1.2 $g \cdot L^{-1}$ was expected in a raceway pond as conducted by Massey University. This study used maximum at 1.2 $g \cdot L^{-1}$ as the worst case and this concentration unit was conversed to volume fraction form as shown in Appendix A. Physical properties (i.e. molar mass, density and transport properties) of seawater and algae assumed to be *Spirulina platensis* species) were defined by using data from handbooks as shown in Table 3.1.

Domain creation

The raceway pond model required five domains: a rotating paddle wheel domain and four stationary pond domains. Rotating domain was specified as immersed solid while other domains contain seawater as a continuous phase and algae cell as spherical a solid dispersed phase.

Table 3.1 Physical properties of materials inside a raceway pond.

Material	Physical property			
	Phase	Particle diameter (mm)	Density ($kg \cdot m^{-3}$)	Dynamic viscosity (Pa·S)
Water	Continuous fluid	-	1030 [31]	0.00131 [31]
Algae	Dispersed solid	47.7×10^{-3} [32,33]	1300 [34]	0.0042 [35,36]

Boundary condition setting

The boundary conditions were essentially set in order to specify the conditions on the surface of the domain. These required boundary conditions were used to solve the conservation of mass and momentum. The equations are solved iteratively as a steady-state. However, this simulation required no inlet and no outlet (batch production) therefore it required only wall boundary condition. Paddle wheel acted role as flow generator and its revolution speed was varied in order to suspend algal cell and obtain flow velocity slightly greater than 0.1 $m \cdot s^{-1}$.

Effect of configuration

Then, a postprocessor was used for the analysis and visualization of resulting solution. This study had to observe the flow pattern as well as the dead zone area, so CFD postprocessor will be resulted to view bulk current velocity and the stagnant zone region. All results available from CFD which will be used to calculate the mixing power requirement.

Velocity profiles

Axial velocity of a paddle wheel affected the velocity profile in the raceway pond. This profile was considered in terms of the dead zone area which has velocity less than 0.1 $m \cdot s^{-1}$. In this step, horizontal XZ plan near the bottom surface (Y = 0.05 m) was focused to observe the velocity profile.

Dead zone areas

For large pond, algae cell can easily sediment in the pond bottom under no sufficient flow. It also can accumulate in the area called “dead spot” or “dead zone”. Because the entire raceway pond needs to achieve velocity greater than 0.1 $m \cdot s^{-1}$, specific region cannot achieve the target velocity was defined to be dead zone. However, this study only focused

on the returned bends of raceway pond where the sedimentation of algal cells usually occurs.

Power requirement

The required power needed for mixing can be provided either by mechanical or through hydraulic means. The power dissipated by a paddle wheel can be simply calculated in term of paddle area and the relative velocity of a paddle wheel as shown in theory chapter.

3.4 New design of raceway pond

In this step, the modification design of large raceway pond was proposed with the aims of eliminating the dead zone and increasing the energy efficiency by especially modification of the configuration of flow rectifiers such as the central baffle and the flow deflector baffle. The detail of this part can be followed in chapter 4. Finally, the recommendations are shown for future work in this area.

CHAPTER 4 RESULTS AND DISCUSSION

Computational Fluid Dynamics (CFD) was used to simulate the seawater flow behavior in a raceway pond in order to design the geometry that can reduce the dead zone area and obtain more energy efficient. In this chapter, the simulation results of the standard configuration and other five design configurations were analyzed and discussed covering the fluid flow pattern, dead zone area and energy requirement.

4.1 Standard and related designs of raceway pond

4.1.1 Standard model

For this research, the standard configuration is a closed-loop recirculation channel that is typically about 0.3 meters in depth. This configuration contains only the straight line central baffle and uses a paddle wheel to recirculate the biomass and growth media (algal cells and seawater). Mixing is achieved through a combination of the effects of the paddle wheel and the interaction of the flowing water with the bottom and side walls of the raceway. Figure 4.1 shows the overview configuration of the standard model and the returned bend.

4.1.2 Central baffle model

This central baffle design or “the island” design is mostly applied in commercial scale to eliminate the dead zone where the flow forms as large eddies after the bends. There are a few public theories to calculate the appropriate size and shape of this area. However, one can easily observe the eddy flow size in CFD simulation. Therefore, this central baffle shape was generated using the results from the standard configuration at the same velocity. The configuration of this design was shown in Figure 4.2.

4.1.3 Flow deflector baffle model

The raceways were operated with flow deflectors around the 180° bends. Including flow deflector baffle in the return channel is an easier way that can guide the flow around bends in order to minimize space and loss. In practice, there are some interests to add the flow deflector baffle more than one baffle at the end of channel. Hence, a number of added baffles were considered in this study as shown in Figures 4.3 and 4.4.

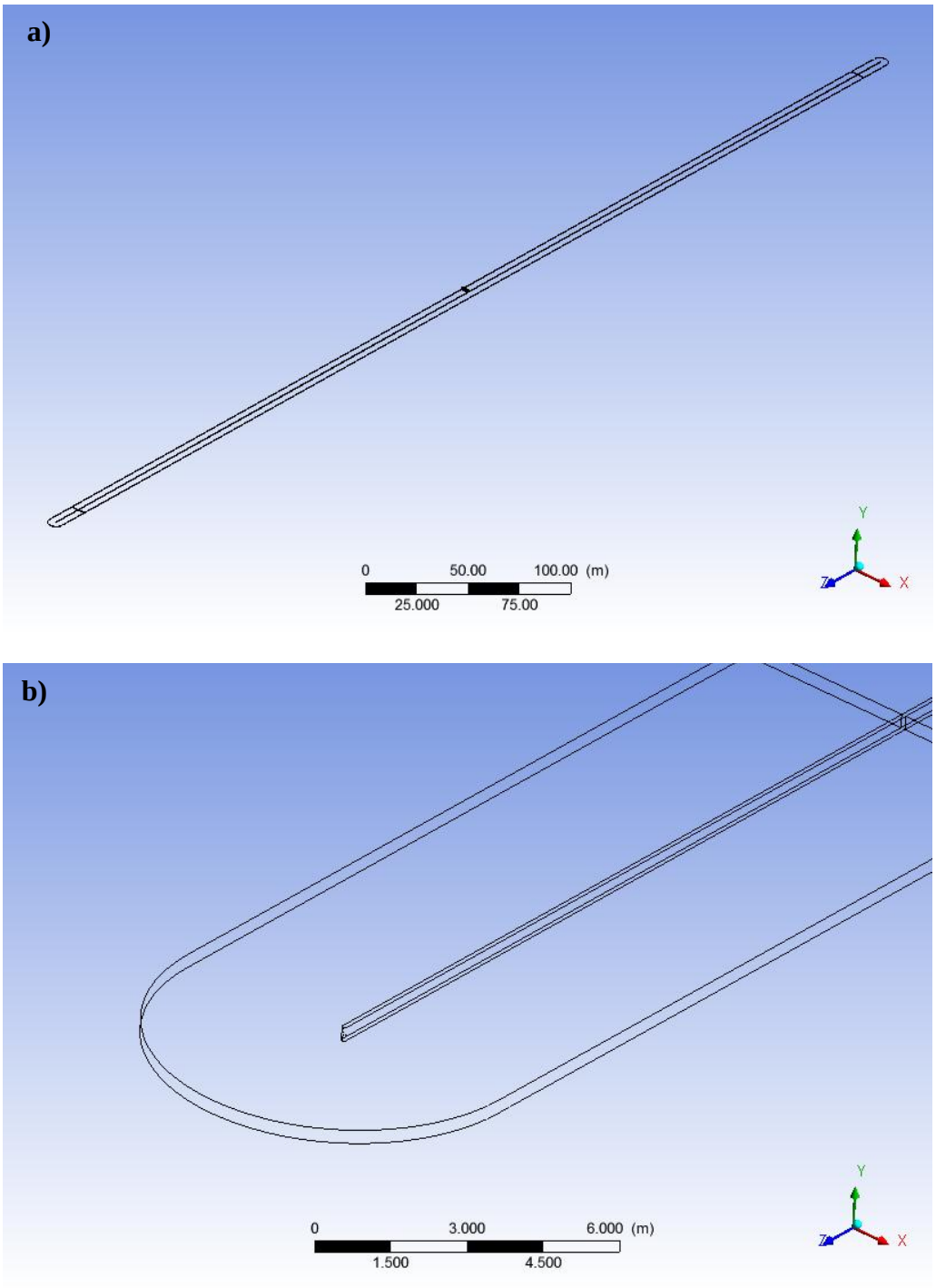

Figure 4.1 Standard configuration of raceway pond a) the overview configuration of the standard model and the paddle wheel location b) the returned bend of the standard configuration.

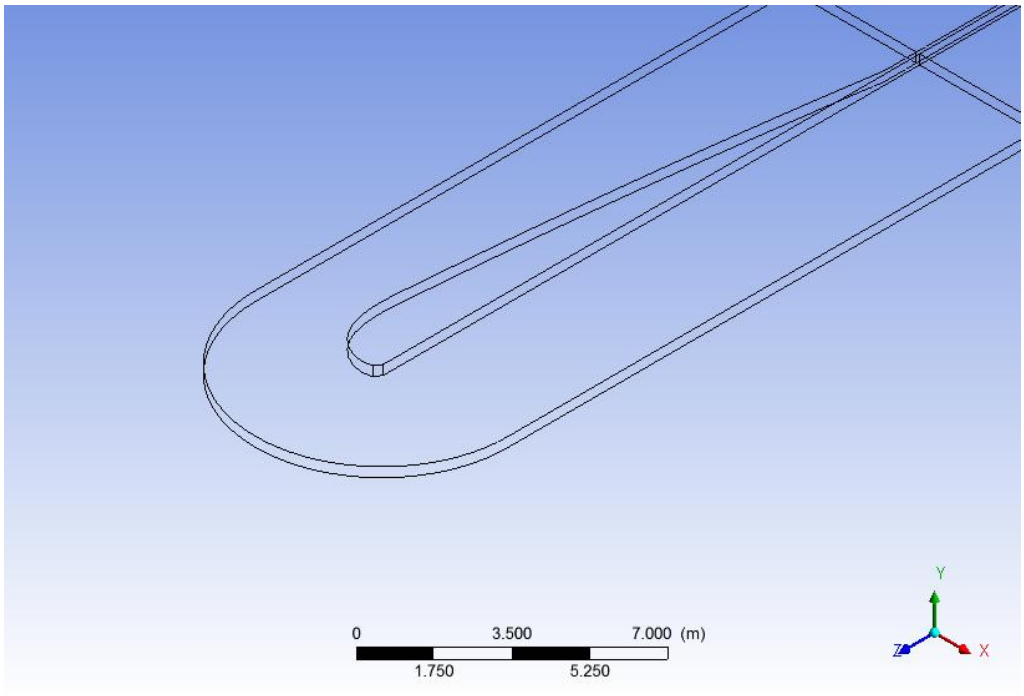

Figure 4.2 Central baffle configuration of a raceway pond.

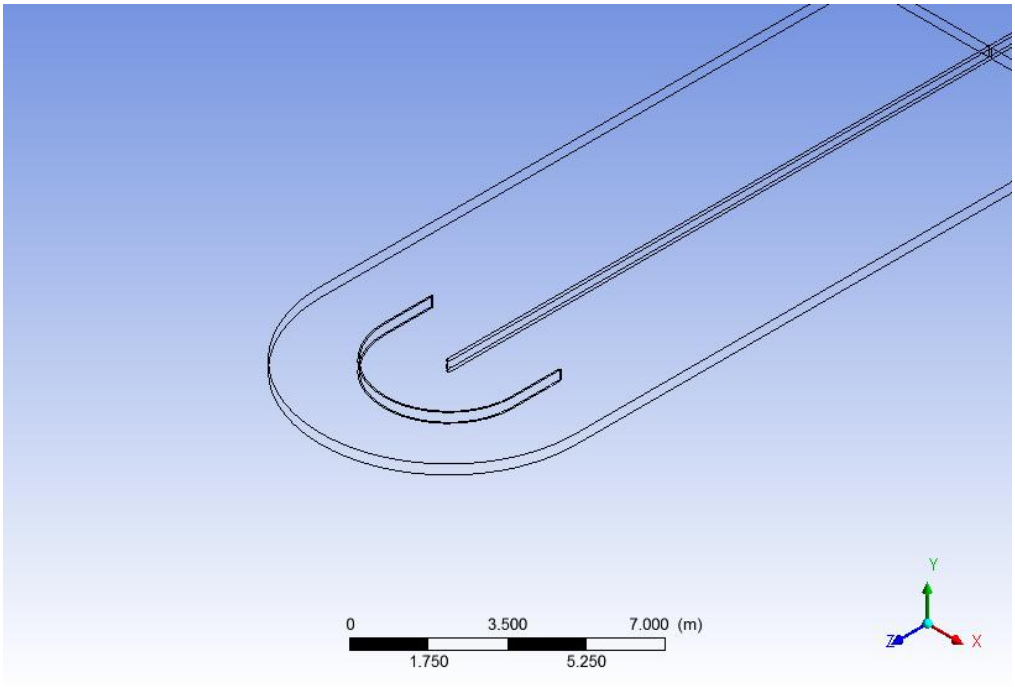

Figure 4.3 Flow deflector baffle configuration of a raceway pond.

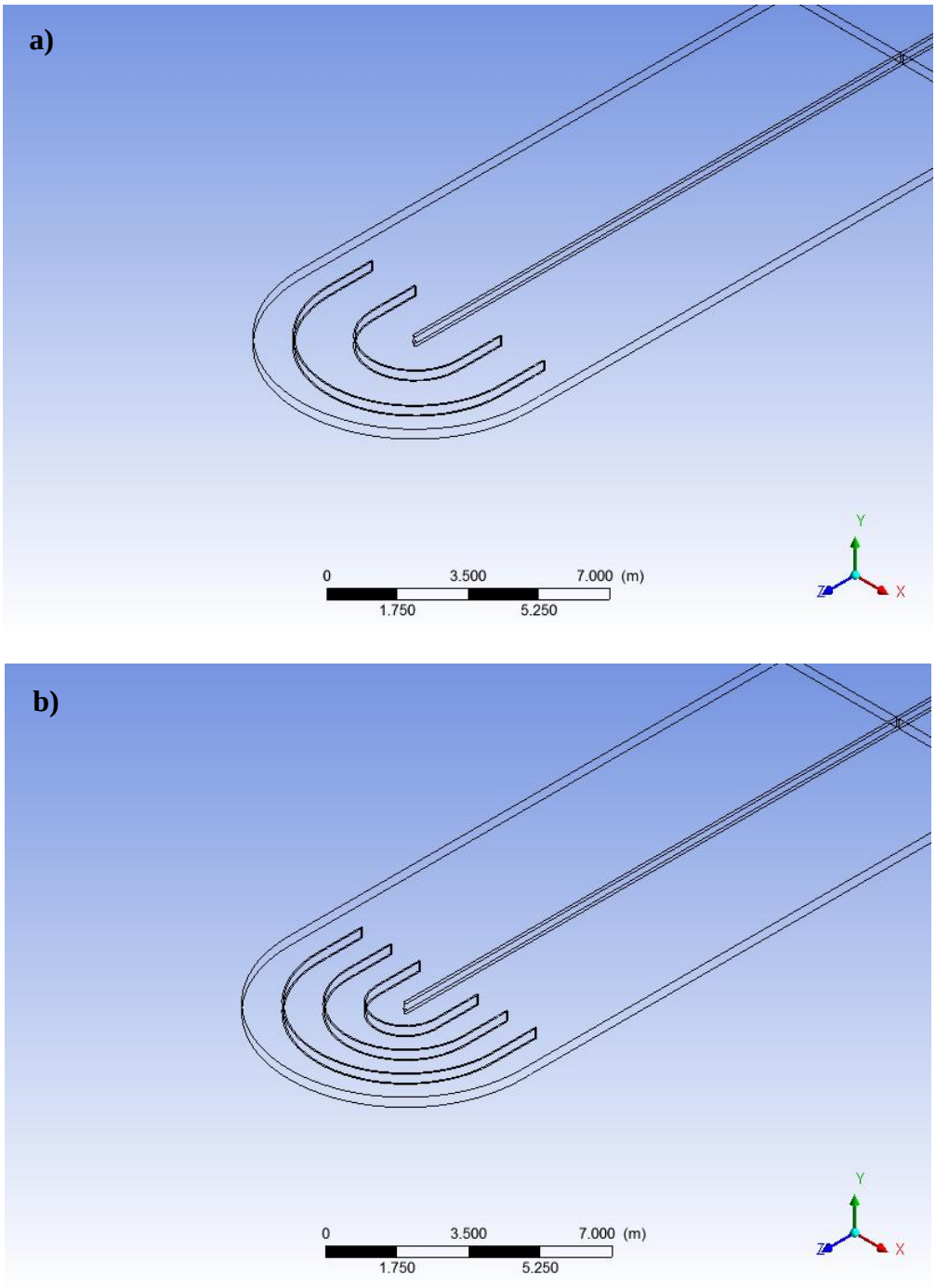

Figure 4.4 Flow deflector baffle series configuration of a raceway pond a) two deflector baffles b) three deflector baffles.

4.2 Geometry mesh generation

Because all of pond designs in this study were the flat and very large configuration and two-phase flow was a complex physical phenomenon and required long time to simulate. The meshing method has to be considered in this study in order to achieve the convergence in the simulation within reasonable simulation results and simulation time.

The mesh size affects both simulation time and accuracy of the solution. Small mesh size takes long simulation time but with higher accuracy while larger mesh size required short time of simulation but less accuracy. For this flat and large configuration, a mesh of each configuration is an importance parameters effect on simulation results. Hence, this work separated the raceway pond into 4 bodies. This can avoid the difference meshing in the central channel of a large raceway while the 2 bend parts of each configuration were meshed in the same condition. This scheme can converse easily if there are input and output interact to the other domains. The central of raceway meshing was defined at maximum face of 0.3 meters as shown in Figure 4.5 hence the mesh number of each configuration in this position was same as the others.

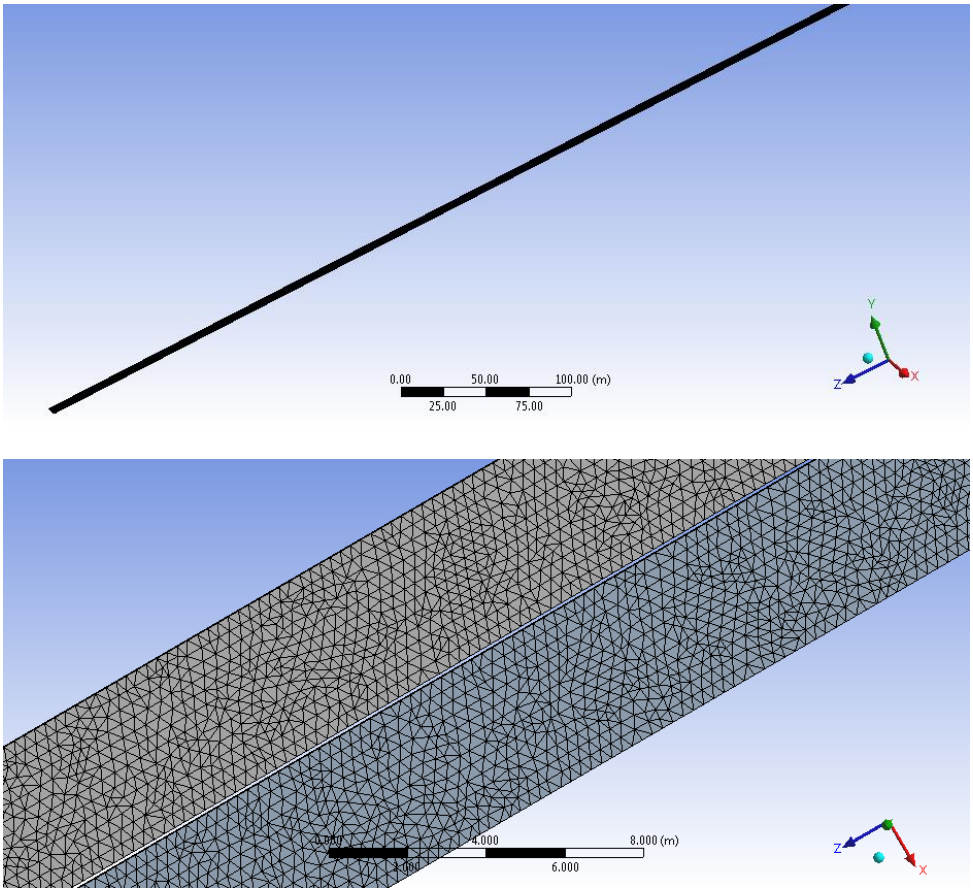

Figure 4.5 Mesh of central body of raceway.

The two bends of raceway (i.e. both side of head and tail) were changed following the configuration design pattern. Difference design means difference in meshing. However, they were meshed by the same conditions and can ensure that each mesh size was similar. The meshed bends of standard, central baffle and flow deflector baffle configurations were shown in Figure 4.6 while their mesh numbers were concluded in Table 4.1.

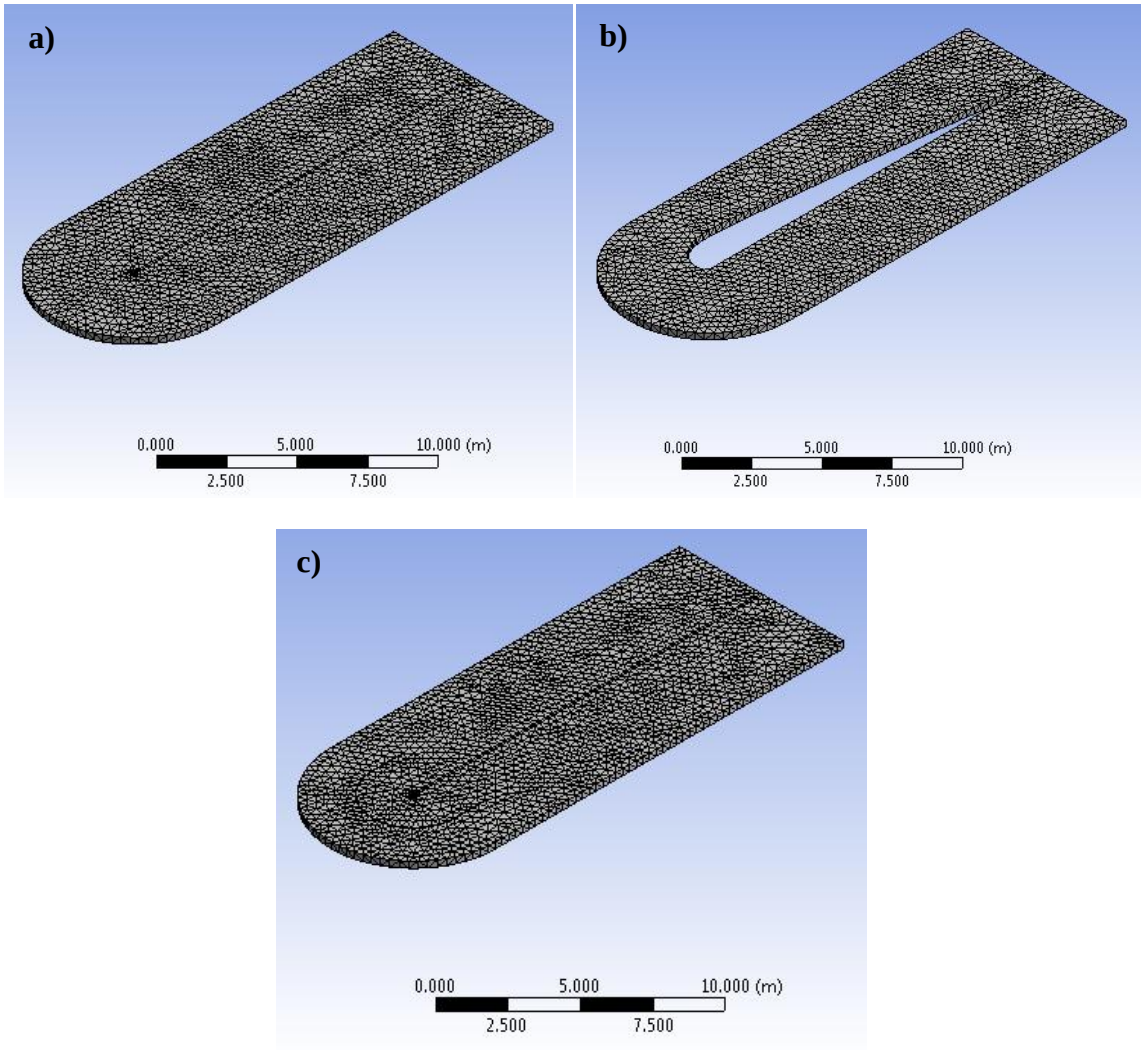

Figure 4.6 Mesh of the returned bend body of raceway a) standard b) central baffle c) flow deflector baffle.

Table 4.1 The statistics of element and node number of each configuration.

Configuration	Elements		Nodes	
Paddle wheel	12993		21452	
	Central body	**Returned bend body**	**Central body**	**Returned bend body**
Standard	344095	21707	114415	7440
Central baffle		18680		6553
Flow deflector baffle		21354		7464
Two deflector baffles		21279		7595
Three deflector baffles		21527		7724

4.3 Simulation results of raceway pond

The raceways were first operated without flow deflectors around the 180° bends. In this raceway pond, seawater flow was firstly generated from the paddle wheel with rotational speed of 35 rpm and continued straightly to channel. Flow pattern was then swerved at the lower bend and continued far into another channel before returned again to enter to paddle wheel. It definitely was a closed loop recirculation channel.

4.3.1 Standard model

As the above mentioned, the standard configuration raceway was firstly operated to observe the flow pattern. The water flow velocity was maintained at the level of slightly greater than 0.1 $m \cdot s^{-1}$ to maintain turbulent mixing by varying revolution of a paddle wheel. As mentioned in chapters 2 and 3, the data from operating experiment suggested flow rate should be in the range of 0.1-0.24 $m \cdot s^{-1}$. Therefore, the rotational speed of a paddle wheel was first varied from 30 to 55 rpm in the standard model. The water flow rate had significant effects on the dead zone area and the power requirement in a raceway pond.

The flow pattern in the standard configuration was predicted from the seawater velocity streamlines shown in Figure 4.7 while Figure 4.8 shows the velocity profile and the dead region of each rotational speed. As expected, the flow was characterized by large eddies formed just after the bends and the central baffle where can cause the flocculation of algae cells. This research concerned especially flow around the returned bends, thus the velocity profiles which shown in this part will focus only the bends.

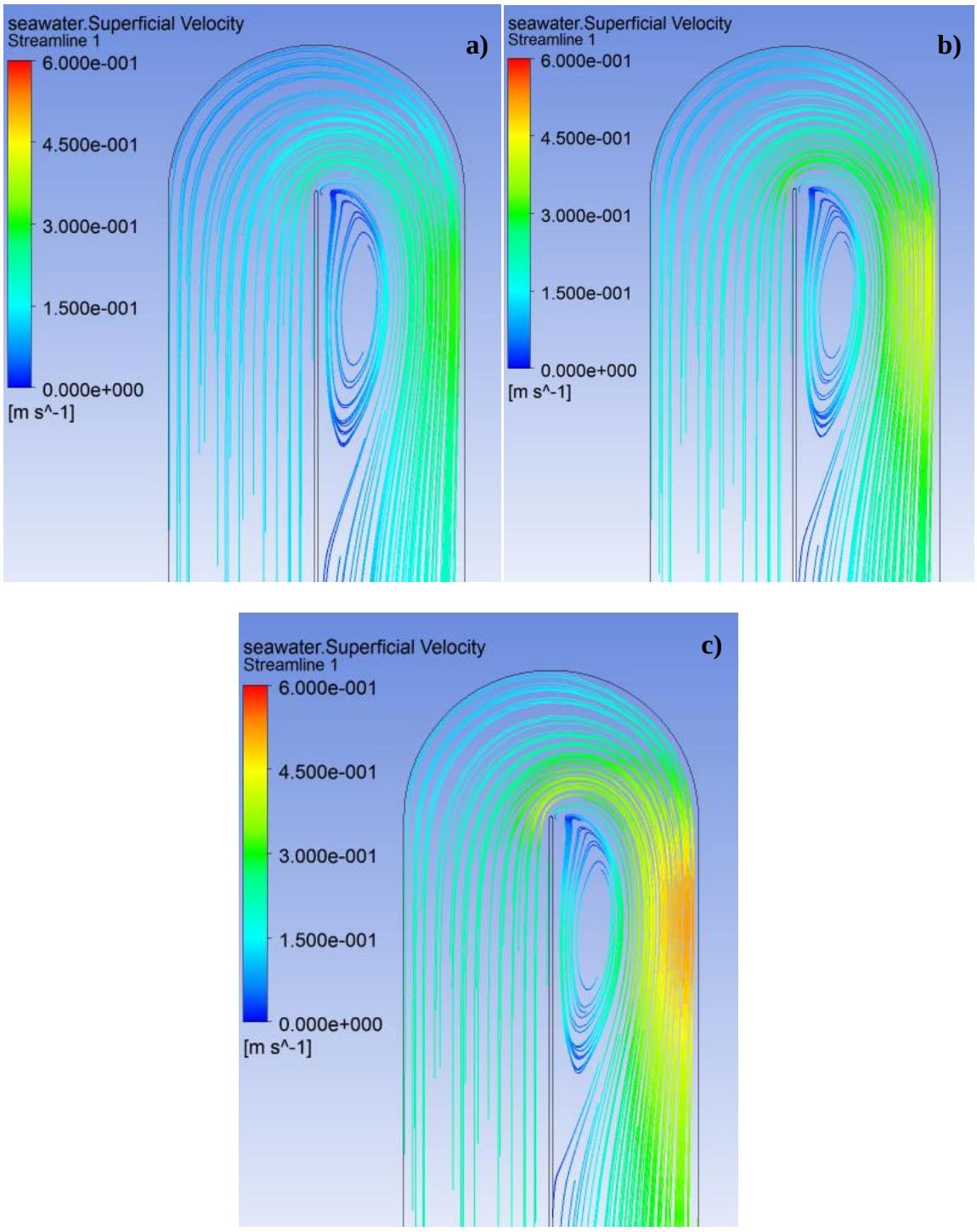

Figure 4.7 Seawater velocity streamline a) rotational speed of 35 rpm b) rotational speed of 45 rpm c) rotational speed of 55 rpm.

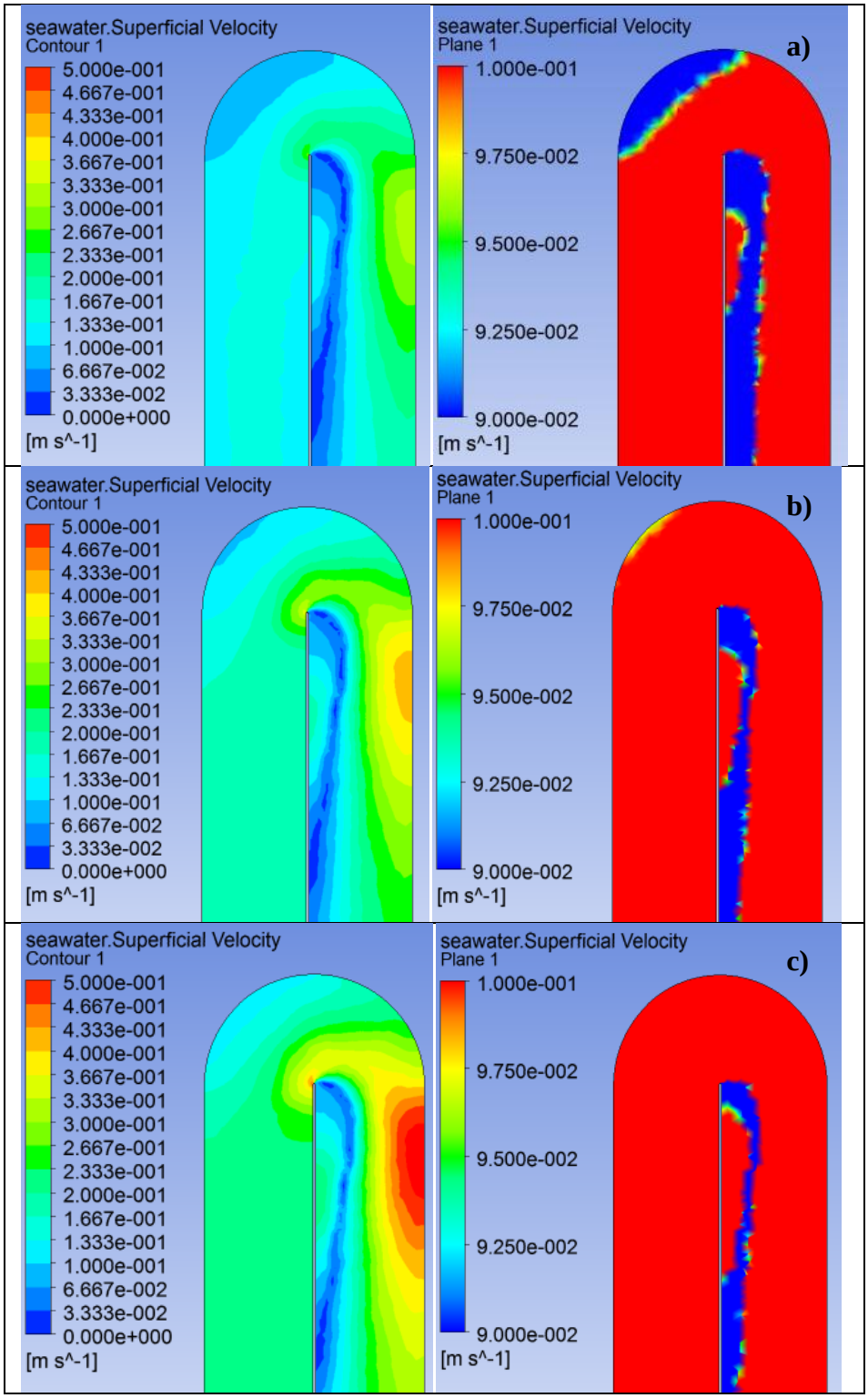

Figure 4.8 Seawater velocity profiles and dead zone area a) rotational speed of 35 rpm b) rotational speed of 45 rpm c) rotational speed of 55 rpm.

This research aims to achieve average velocity by about 0.12 $m \cdot s^{-1}$. This average velocity also included the paddle wheel location where can generate the high velocity at least 0.1 $m \cdot s^{-1}$ in a raceway pond (accept the area of bend and after bend). To achieve this average velocity by about 0.12 $m \cdot s^{-1}$, the number of revolution of a paddle wheel can be found from relation between rotational speed and velocity as shown in Figure 4.9. For the standard configuration, 32 rpm was applied to perform flow at velocity of 0.12 $m \cdot s^{-1}$. Therefore, this case will be a base case for comparing between the standard case and the other cases in terms of the velocity profile, energy consumption and dead zone reduction. Figure 4.10 shows the dead zone areas which occurred in the standard configuration with 32 rpm of the paddle wheel operation.

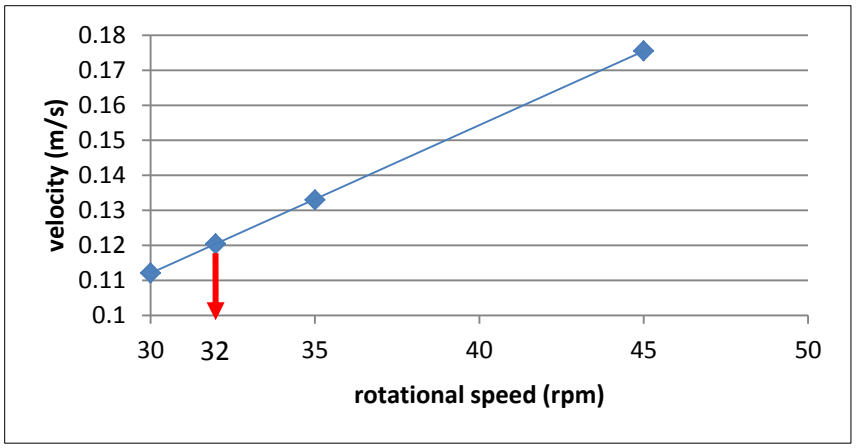

Figure 4.9 Average velocities with different rotational speed of a paddle wheel for the standard configuration.

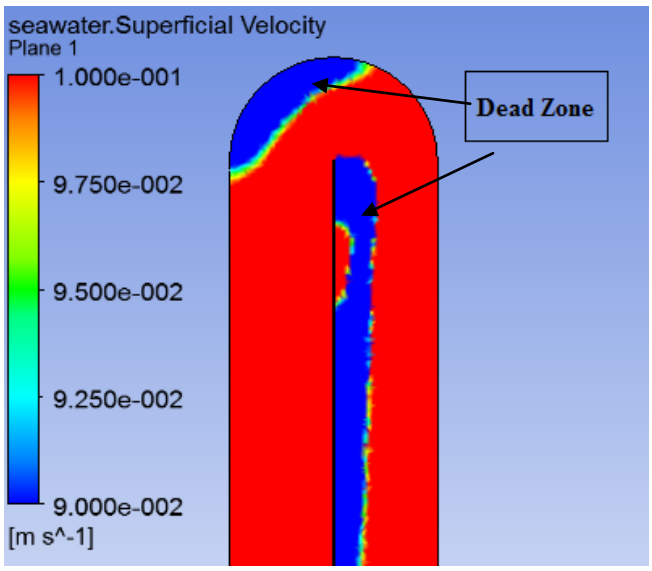

Figure 4.10 Dead zone areas which occurred in the standard configuration with 32 rpm of the paddle wheel operation.

4.3.2 Central baffle model (Island model)

According to the significant dead zone in the standard model, this central baffle configuration was designed to eliminate the dead region after the bends. There was two dead zone occurred in the bend area in Figure 4.10. One located at the bend curved and another one located at the after bend (behind the central baffle). Moreover, in order to remove all of these two dead spots, this model required the high seawater flow velocity up to 0.18 $m \cdot s^{-1}$ in the simulation. That means the high rotational speed of paddle was required to eliminate all of dead zone at the bends. However, this configuration also varied the rotational speed of a paddle wheel to see trends of velocity, power requirement and percentage of the dead region. The varying results of this model are shown in comparing issue.

For the average seawater velocity of 0.12 $m \cdot s^{-1}$, this configuration required rotational speed of 31 rpm. Its velocity profile is shown in Figure 4.11 a). The central baffle configuration showed a good result of handle the dead spot on the back side of the central baffle. However, as shown in Figure 4.11 b), there was one of the dead spot still on the left of the bend curved. Its shape was same as the standard configuration. The reason came from the flow around the bend is the vortex flow. This flow was the highest speed where the radius of curvature is the smallest while the slowest speed occurred at the largest radius [37]. The higher pressure near the outer bend is accompanied by decreasing the seawater speed, and the lower pressure near the inner bend by increasing the water speed. All of these phenomena are consistent with Bernoulli's principle.

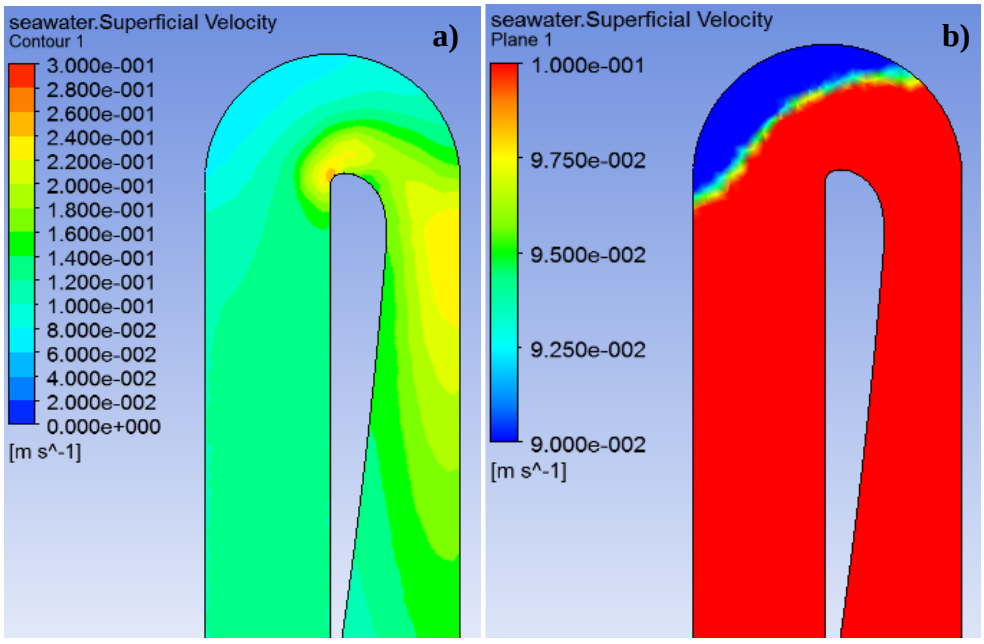

Figure 4.11 Central baffle configuration with 31 rpm of the paddle wheel operation a) velocity profile b) dead zone area.

4.3.3 Flow deflector baffles model

This configuration was able to formulate a curved zone of accelerated flow. As mentioned in chapter 2, the rate of constriction of the curved zone is sufficient to reduce the velocity below that causing solids deposition on the back side of the central baffle.

From the simulation results, the one flow deflector baffle configuration required average velocity greater than 0.18 $m \cdot s^{-1}$ to remove the dead zone at the bends and the inner of baffle while the dead spot still existed on the back side of the central baffle. Moreover, this configuration required rotational speed at 30 rpm to maintain average velocity of 0.12 $m \cdot s^{-1}$. That means this model required lower energy input than the standard and central baffle configurations. Figure 4.12 a) shows the velocity profile of accelerating flow and Figure 4.12 b) indicates the result of the dead spot position which occurred in a raceway pond.

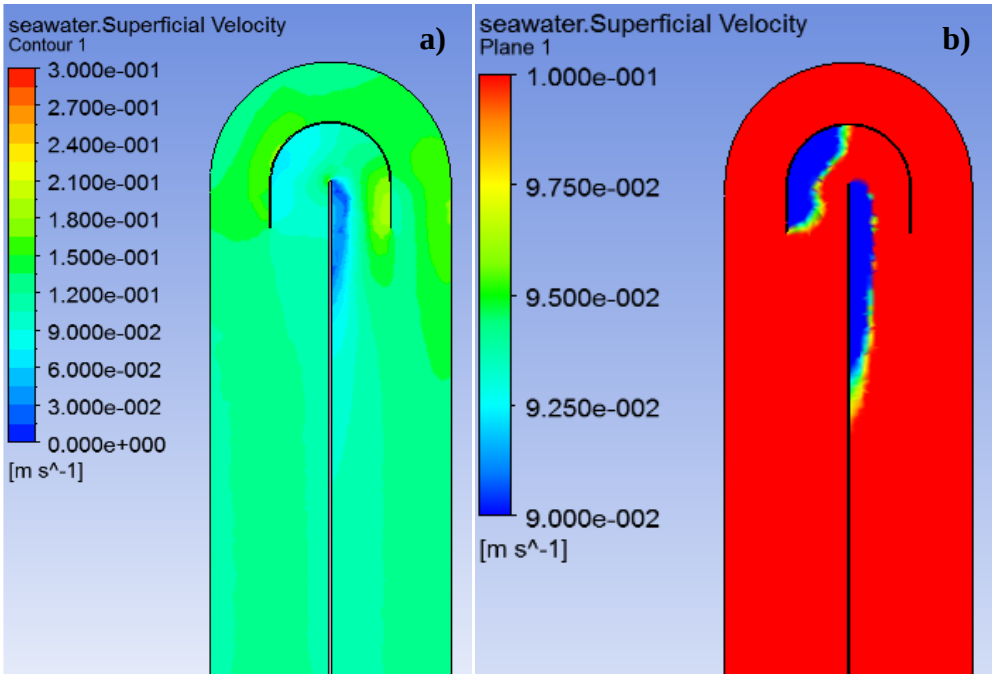

Figure 4.12 Flow deflector baffle configuration with 30 rpm of the paddle wheel operation a) velocity profile b) dead zone area.

Recently, most of open pond cultivations applied the flow deflector baffle more than one unit. They used two or three baffles in series to reduce the dead zone areas. From the simulation results in Figures 4.13 and 4.14, one can notice that, at the same rotational speed, both of the flow deflector two and three deflector baffles provided the same average velocity and also the energy requirement as the one baffle configuration. On the other hand, this could offer more efficient in terms of solids deposition area reducing. Figure 4.15 illustrates that the number of Flow deflector baffle related to the reducing of the dead zone.

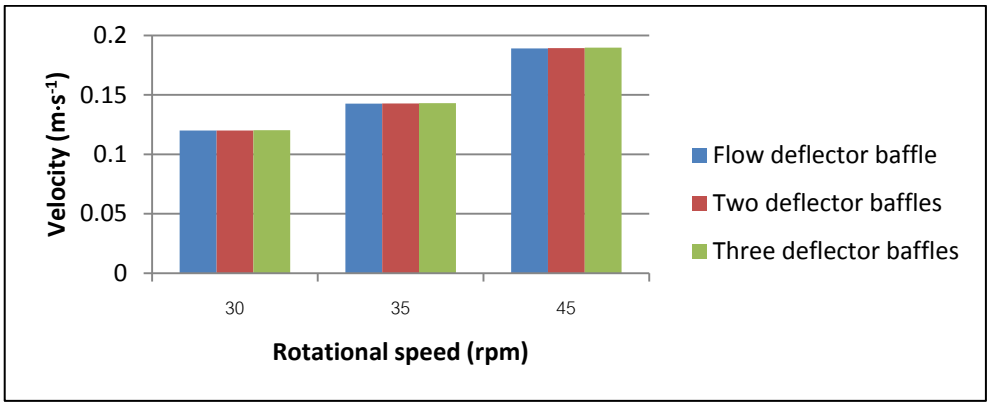

Figure 4.13 Velocities of deflector baffle in series with different rotational speed.

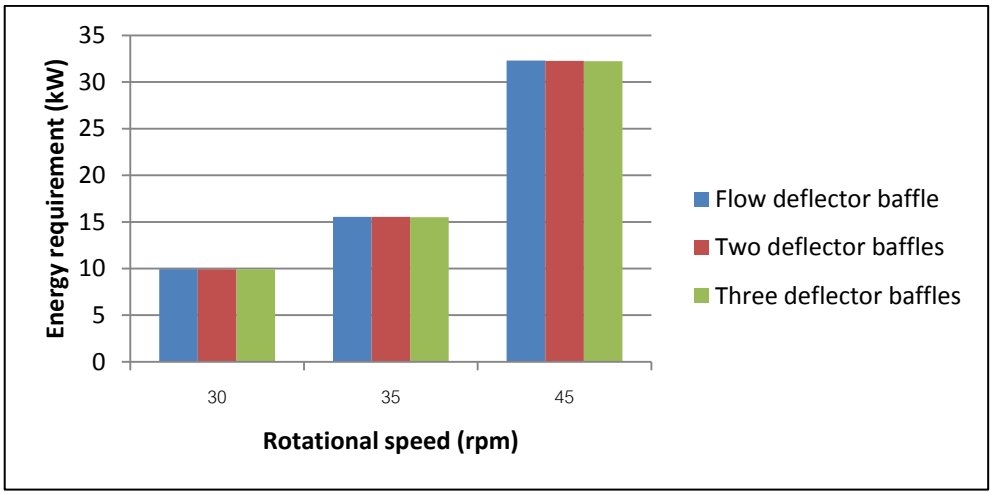

Figure 4.14 Energy requirement of deflector baffle in series with different rotational speed.

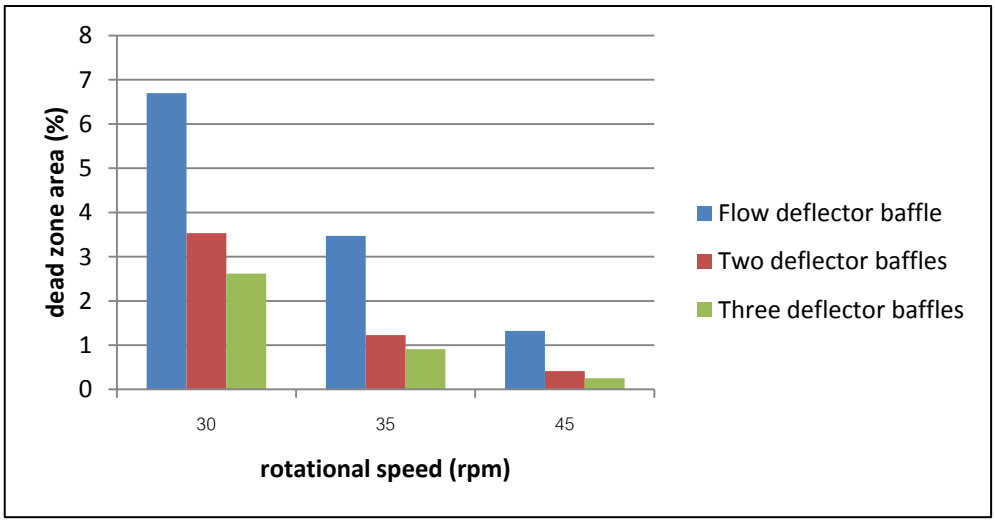

Figure 4.15 Percentage of dead zone of deflector baffle in series with different rotational speed.

From the above results, three deflector baffles model was selected to compare with other configurations (i.e. the standard configuration and the central baffle) because of its benefit. This configuration required rotational speed of 30 rpm to maintain average velocity of 0.12 $m \cdot s^{-1}$ but area of the dead spot was reduced from 6.7 to 2.6% of the two bend areas when the three deflector baffles was compared to the one baffle model. Figure 4.16 shows the comparison of the dead spot area between flow deflector baffle, two deflector baffles and three deflector baffles.

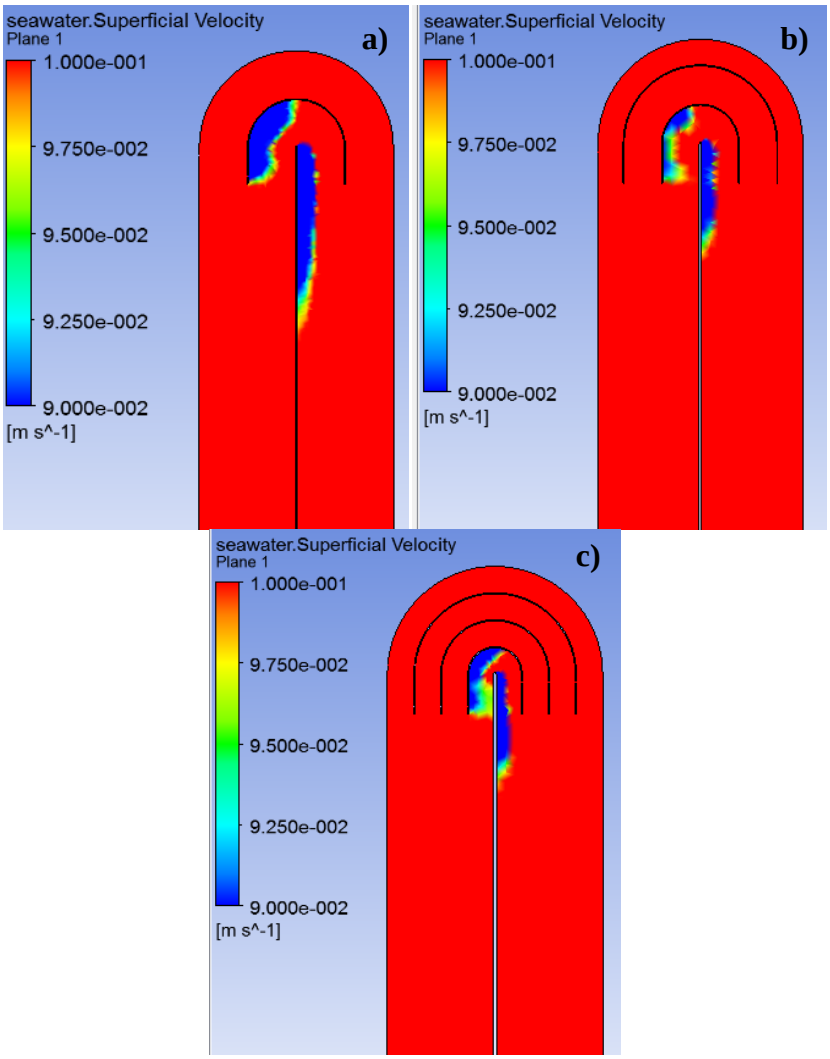

Figure 4.16 Comparison of the dead spot area between a) flow deflector baffle b) two deflector baffles and c) three deflector baffles.

In conclusion, introducing more deflector baffles at the bend was used to guide the flow around the bend and also decrease loss from pressure difference between radius of the outer bend and inner bend. It affected the waterflow velocity of the inner and outer of bend is

slightly different from each other. Thus, this configuration offered more uniform waterflow velocity than other models.

4.4 Configurations comparison

The rotational speed of a paddle wheel in this study was varied from 30, 35 and 45 rpm for all of configurations; the standard, central baffle and three deflector baffles. Two model configurations were selected and compared with the standard configuration in three main issues 1) average velocity, 2) energy requirement provided at the same velocity, and 3) percentage of the dead zone. All of these main factors can help in decision stage of modified model.

The rotational speed influenced directly on average velocity in a raceway pond as shown in Figure 4.17. Three deflector baffles supplied the higher velocity than the standard and the central baffle configuration at the same of rotational speed of a paddle wheel. The trend of increasing velocity definitely followed the increasing of the number of revolution speed. However, at the same rotational speed, the results did not imply that paddle wheel required the same energy input. Figure 4.18 was created to review the trend of energy consumption of each model. It showed a good agreement with Figure 4.17 in terms of the energy input, three deflector baffles series required less energy input than the others to achieve the same velocity.

According to "The power demand of a traditional paddle wheel is about 600 W for a 100 m^2 pond" [38], this study fixed the total surface size about 5,000 square meters of raceway pond hence the paddle power needed for 5,000 m^2 should approximately be in the range of 30,000 W or 30 kW. The power required by a paddle wheel can be calculated as shown in appendix C.

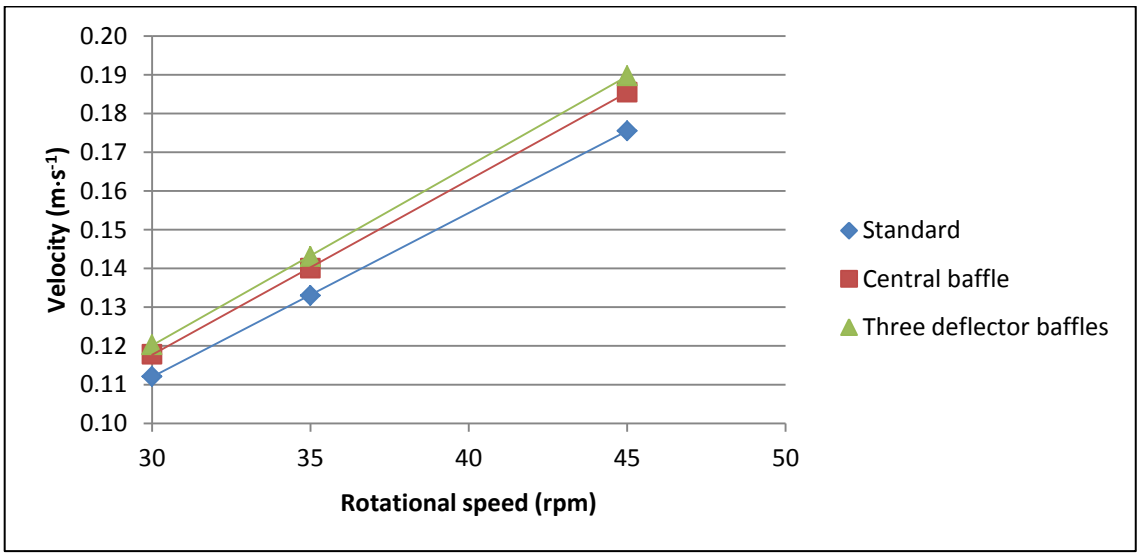

Figure 4.17 Comparison of velocity varied by rotational speed.

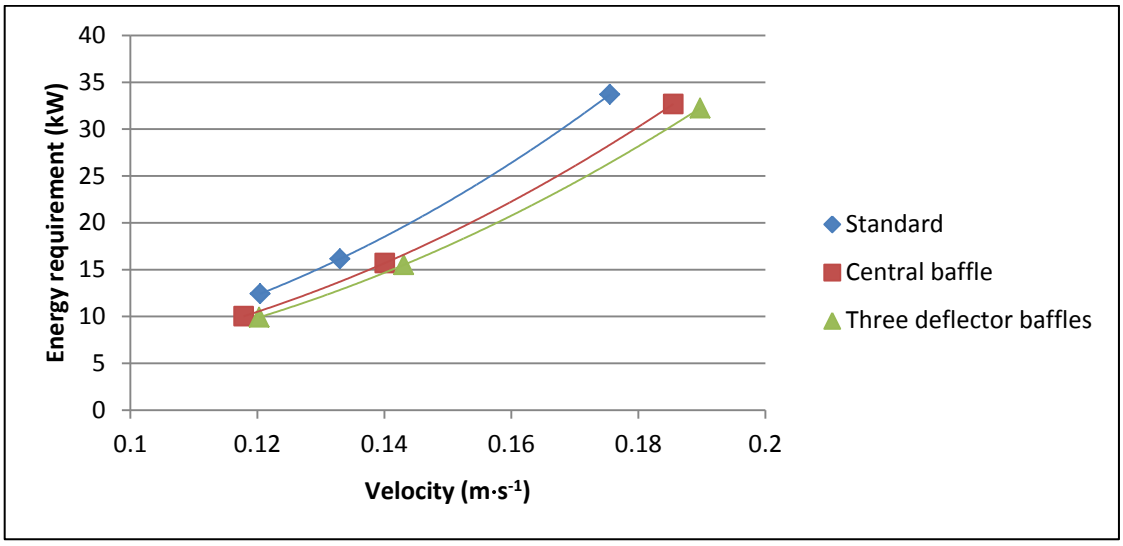

Figure 4.18 Comparison of energy consumption related to velocity.

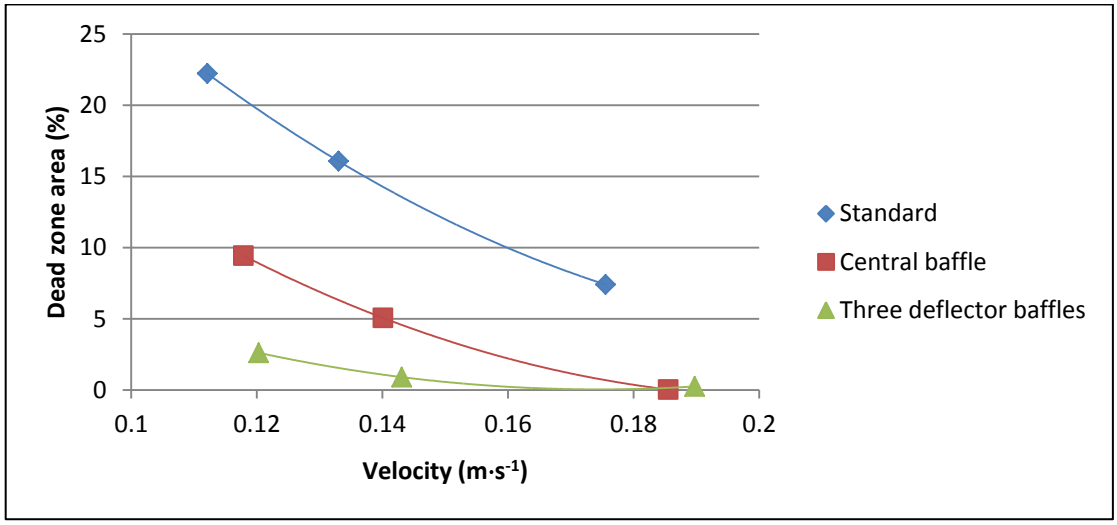

Figure 4.19 Comparison of the dead zone area percentage related to velocity.

In addition, Figure 4.19 clearly promotes to use three deflector baffles series in a raceway pond system because this configuration offers the lowest percentage of the dead zone area. Even though, the central baffle model provided a better result of the dead zone area reducing over the three deflector baffles at high velocity greater than 0.185 $m \cdot s^{-1}$, the operating condition of raceway system still concentrated on region of low energy consumption. Therefore, the proposed three deflector baffles was the good configuration that require less energy to achieved target velocity and also supplied a minimum dead spot region to avoid solids deposition in the raceway pond.

4.5 Modified configuration

This modified model can be created from the combination between three deflector baffles and central baffles concept. Especially, the three deflector baffles design was the main interest to improve reasonable.

The first improved configuration shows in Figure 4.20 a). This figure combined the central baffle and the three deflector baffles design to eliminate the dead zone area. However, this improved model cannot remove all of dead region around the bends of raceway pond despite increased average seawater velocity up to 0.14 $m \cdot s^{-1}$ as shown in Figure 4.20 b). Therefore, the increase in velocity of seawater before swerve around the bends is needed. This approach can be done by narrowing the waterflow area to force the flow moves faster at the bends.

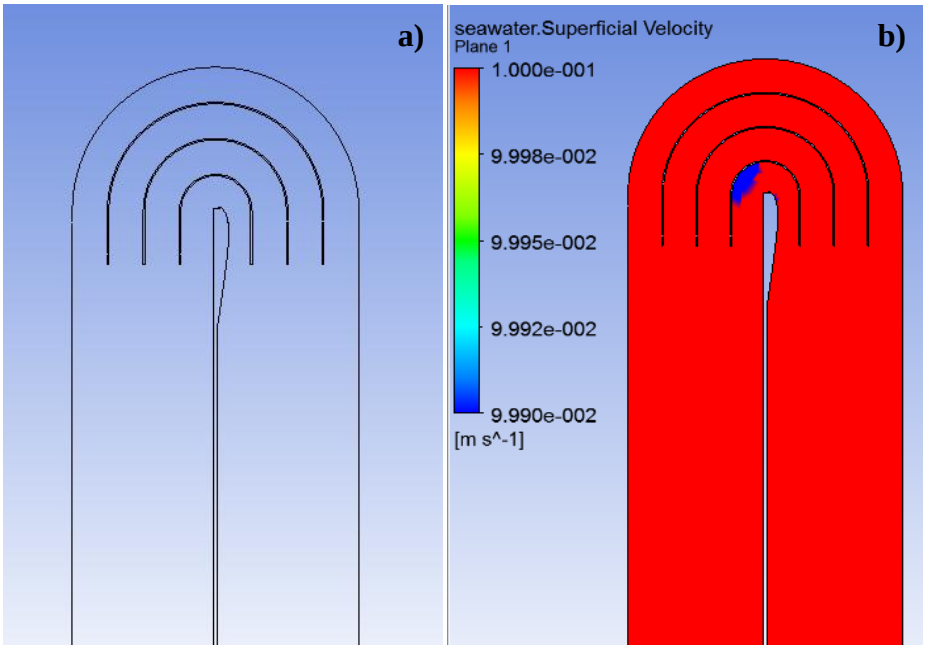

Figure 4.20 Modified configuration of raceway pond a) geometry b) dead zone area with 35 rpm of the paddle wheel operation

Figure 4.21 was improved from the previous one. The central baffle of this model was improved by decreasing the waterflow area before swerve around the bends with the baffles style. The simulation was then carried out in order to compare the energy consumption and the dead zone area with the existing standard and three deflector baffles configuration. The velocity profiles inside all of models are shown in Figure 4.22 while Figure 4.23 illustrates the areas of dead zone which occurred in each configuration. The average velocity of 0.14 $m \cdot s^{-1}$ was selected to compare these three configurations.

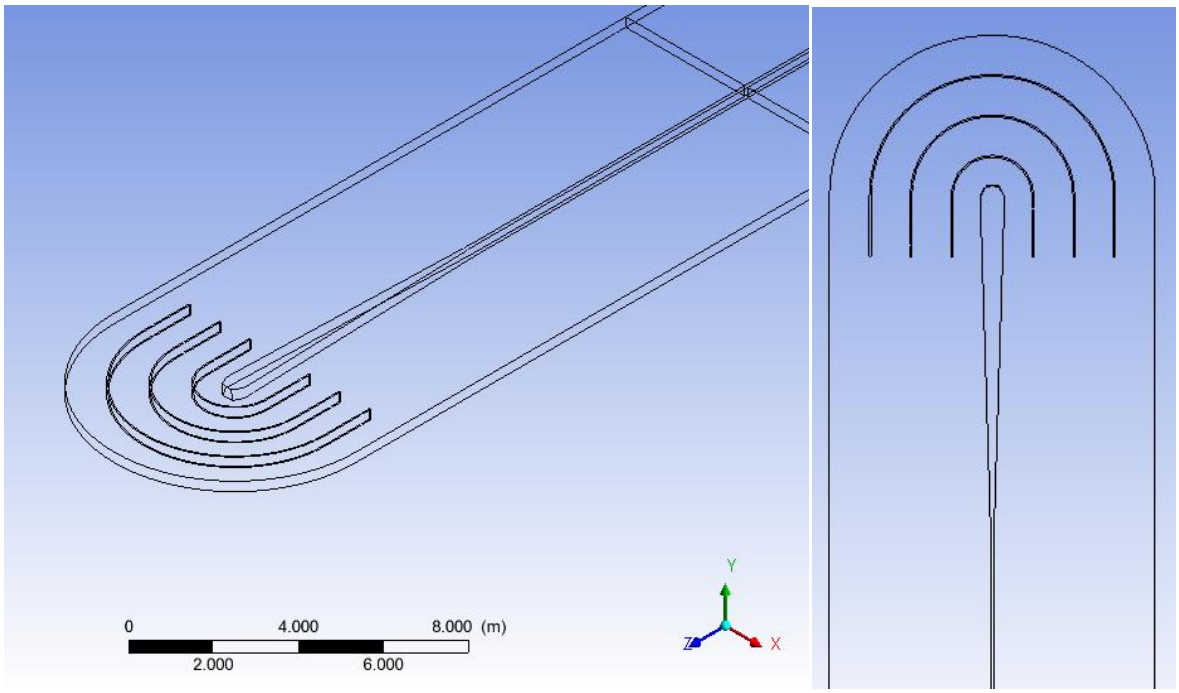

Figure 4.21 New modified configuration of raceway pond

The configuration of modified model can force the flow pattern of seawater to change gradually. This was a cause of decreasing the pressure drop. The new configuration provided better results of uniform velocity than the standard model and no eddy formation after the returned bends as all results shown in Table 4.2 and the bellowing figures. Therefore, the modified configuration gives a significant improvement in the issues of the energy requirement and the dead zone reduction.

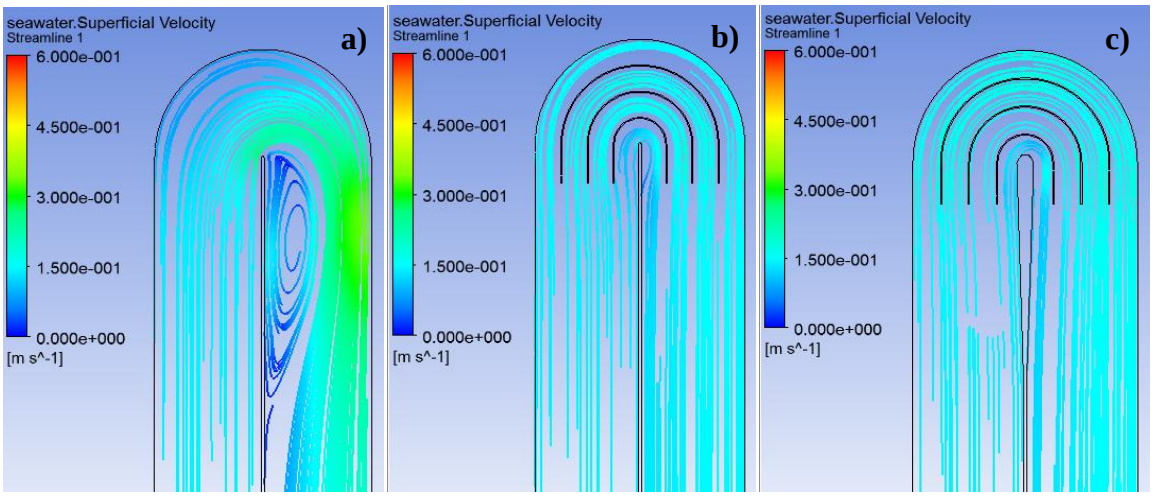

Figure 4.22 Comparison of velocity profile in a) standard b) three deflector baffles and c) modified configuration of raceway pond

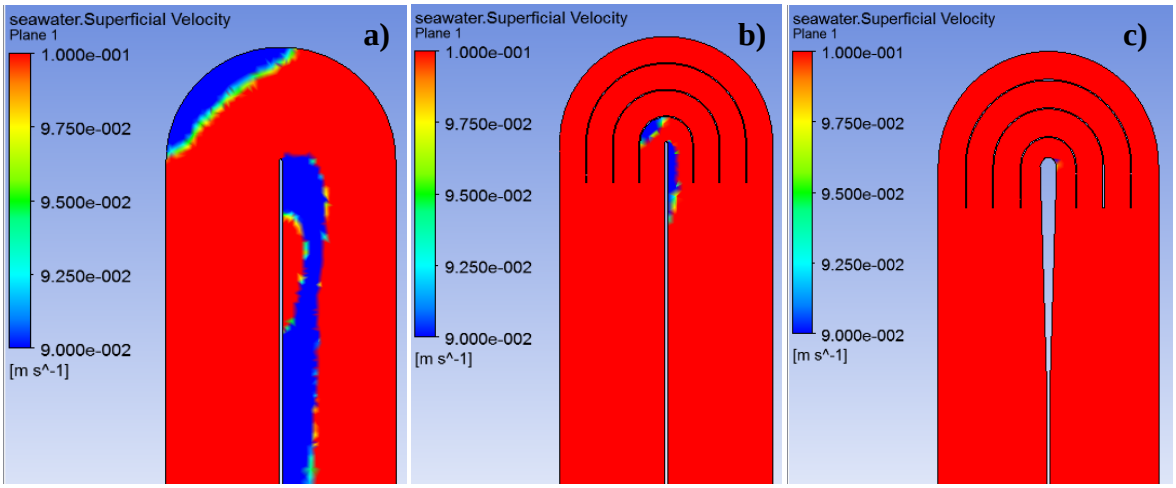

Figure 4.23 Comparison of dead zone area inside a) standard b) three deflector baffles and c) the modified configuration.

The comparative results show that configuration adjustment can reduce the dead zone and provide more energy efficient input. The comparison of the configuration between the standard design results and the proposed design results can be concluded in Table 4.2. The results show that central baffle, flow deflector baffle, two and three deflector baffles and modified configurations applied the rotational speed of paddle wheel and consumed energy less than the standard configuration. Preferably, the modified configuration can consume energy less than other configuration and eliminate all of the dead area at bends.

Table 4.2 Comparison of overall configuration results at approximate velocity of 0.14 $m \cdot s^{-1}$

Configuration	Rotational Speed (rpm)	Velocity ($m \cdot s^{-1}$)	Energy requirement (kW)	Dead zone area (%)
Standard	37	0.141	19.00	14.23
Central baffle	35	0.140	15.71	5.07
Flow deflector baffle	35	0.143	15.54	3.47
Two deflector baffles	35	0.143	15.55	1.23
Three deflector baffles	35	0.143	15.52	0.91
Modified	35	0.146	15.50	0.00

CHAPTER 5 CONCLUSIONS AND RECOMMENDATIONS

5.1 Conclusions

This research studied the designs of the large raceway pond covering the energy consumption and the dead spot area. The two-phase model (solid-liquid) was developed using ANSYS program in order to study and visualize the flow pattern of seawater and the position of dead spot in the returned bends of raceway pond. The focused design models in this work were the central baffle model and flow deflector baffle to compare with the standard model of raceway pond. All configurations was modeled for a total surface area of 0.5 ha (5000 m^2) by 8 m width and 0.3 m height fixed. The algae species was assumed to be *Spirulina platensis*, culturing at 20°C of seawater.

The simulation results showed that, the rotational speed of a paddle wheel directly affected the seawaterflow velocity. However, the same rotational speed did not imply a paddle wheel would require the same energy input. Hence, all of models had to be compared at the same velocity. The results of each simulation showed three deflector baffles provided the best points of the energy consumption and the reducing dead zone area. Therefore, this model would be the main interest to improve a new configuration. When compared the standard model and the modified model at velocity of 0.14 $m \cdot s^{-1}$, it could reduce the energy requirement by about 18.4% and eliminate all of the dead area at bends.

5.2 Recommendations

1. This modified configuration can be used as a guide for future design of large raceway pond for total surface area of 0.5 ha (5000 m^2) especially the bend design, scale up should be studied for future works.

2. The width to length ratio of raceway can affect to the velocity profile and the dead zone area size. Various ratios are recommended for the designs which do not fix width or length of raceway pond.

3. The exactly algae species can be defined to studies on algae growth factor using growth model.

4. An alternative to a paddle wheel such as gas lift mixing affects to the flow phenomena and the energy consumption. This mixing system can be analyzed in terms of the energy consumption and compared to the paddle wheel mixing.

REFERENCES

1. Johnson, D. A., 1988, **An Outdoor Test Facility for the Large-Scale Production of Microalgae**, SERI/TP-231-3325, Golden, Colo.: Solar Energy Research Institute.

2. Whittaker, R. H., 1975, **Communities and Ecosystems**, 2nd edition, New York: MacMillian Publishing Co.

3. Richmond, A., and Vonshak, A., 1978, *Spirulina* culture in Israel. ***Arch. Hydrobiol***. 11:274–280.

4. Borowitzka, M. A., 2005, Culturing microalgae in outdoor ponds. In: Andersen, R. A., ed. ***Algal cuturing techniques***. Elsevier Academic Press, San Diego, California, pp. 205–218.

5. Borowitzka, M. A., 1999, "Commercial production of microalgae: Ponds, tanks, tubes and fermenters", **Journal of Biotechnology**, 70: 313–321.

6. Castenholz, R. W., 1989, Subsection III. Oscillatoriales. In: Stanley, J. T., Bryant, M. P., Pfenning, N., and Holt, J. G., eds. ***Bergey's Manual of Systematic Bacteriology***. Vol. 3, p.1771.

7. Belay, A., Ota, Y., Miyakawa, K., and Shimamatsu, H., 1994, Production of high quality *Spirulina* at Earthrise Farms. In: Phang, S. M., Lee, K., Borowitzka, M. A., and Whitton, B., eds. ***Algal Biotechnology in the Asia-Pacific Region***. Institute of Advanced Studies, University of Malaya, Kuala Lumpur, pp. 92–102.

8. Fox, R. D., 1996, ***Spirulina:*** **Production and Potential**. Edisud, Aix-en-Provence, France, 232 pp.

9. Belay, A., 1997, **Mass culture of *Spirulina* outdoors: The Earthrise Farms experience**. In: Vonshak, A., ed. *Spirulina platensis (Arthrospira): Physiology, Cell-biology and Biochemistry* Taylor & Francis, London, pp. 131–158.

10. Borowitzka, L. J., and Borowitzka, M. A., 1989, b-Carotene (provitamin A) production with algae. In: Vandamme, E. J., ed. ***Biotechnology of Vitamins, Pigments and Growth Factors***. Elsevier Applied Science, London, pp. 15–26.

11. Schlipalius, L., 1991, "The extensive commercial cultivation of *Dunaliella salina"*, **Bioresource Technology**, 38:241–243.

12. Ben-Amotz, A., 1999, Production of beta-carotene from *Dunaliella*. In: Cohen, Z., ed. ***Chemicals from Microalgae***. Taylor & Francis, London, pp. 196–204.

13. Gummert, F., Meffert, M. E., and Stratmann, H., 1953, Nonsterile large-scale culture of *Chlorella* in greenhouse and open air. In: Burlew, J. S., ed. ***Algal Culture. From Laboratory to Pilot Plant***. Carnegie Institution of Washington, Washington, D.C., pp. 166–176.

14. Tsukada, O., Kawahara, T., and Miyachi, S., 1977, Mass culture of *Chlorella* in Asian countries. In: Mitsui, A., Miyachi, S., San Pietro, A., and Tamura, S., eds. ***Biological Solar Energy Conversion***. Academic Press, New York, pp. 363–365.

15. Kawaguchi, K., 1980, Microalgae production systems in Asia. In: Shelef, G., and Soeder, C. J., eds. ***Algae Biomass Production and Use***. Elsevier/North Holland Biomedical Press, Amsterdam, pp. 25–33.

16. Bubrick, P. 1991, "Production of astaxanthin from *Haematococcus*", **Bioresource Technology**, 38:237–239.

17. Olaizola, M., 2000, "Commercial production of *astaxanthin* from *Haematococcus pluvialis* using 25,000-liter outdoor photobioreactors", **Journal of Applied Phycology**, 12:499–506.

18. Oswald, W. J., 1988, Large-scale algal culture systems (engineering aspects). In: Borowitzka, M. A., and Borowitzka, L. J., eds. ***Micro-Algal Biotechnology***. Cambridge University Press, Cambridge, pp. 357–394.

19. Kaushik, B. D., 1998, Use of cyanobacterial biofertilizers in rice cultivation: A technology improvement. In: Subramanian, G., Kaushik, B. D., and Venkatamaran, G. S., eds. ***Cyanobacterial Biotechnology***. Oxford & IBH Publishing Co, New Delhi, pp. 211–222.

20. Bosca, C., Dauta, A., and Marvalin, O., 1991, "Intensive outdoor algal cultures: How mixing enhances the photosynthetic production rate", **Bioresource Technology**, 38: 185–188.

21. Laws, E. A., Terry, K. L., Wickman, J., and Chalup, M. S., 1983, "A simple algal production system designed to utilize the flashing light effect", **Biotechnology Bioengineering**, 25:2319–2335.

22. Richmond, A., 1986, Outdoor mass culture of microalgae. In: Richmond, A., ed. ***CRC Handbook of Microalgal Mass Culture***. CRC Press, Boca Raton, Florida, pp. 285–329.

23. Perry, R., Green, D. and Maloney, J., 1997, **Perry's Chemical Engineer's Handbook**. (McGraw-Hill).

24. Weissman, J. C., and R. P. Goebel, 1987, **Design and Analysis of Microalgal Open Pond Systems for the Purpose of Producing Fuels**, SERI/STR-231-2840, Golden, Colo.: Solar Energy Research Institute.

25. Dodd, J. C., 1986, Elements of pond design and construction. In: Richmond, A., ed. ***CRC Handbook of Microalgal Mass Culture***. CRC Press, Boca Raton, Florida, pp. 265–283.

26. Shimamatsu, H., and Tominaga, Y., 1980, **Apparatus for Cultivating Algae**. U.S. Patent Office, patent no. 4217728.

27. Shimamatsu, H., 1987, A pond for edible *Spirulina* production and its hydraulic studies. ***Hydrobiologia*** 151/152:83–89.

28. ANSYS Technology, CFX-12 User Manual, 2009, Harwell, United Kingdom.

29. Wikipedia, **Buoyancy** [Online], Available: http://en.wikipedia.org/wiki/Buoyancy [20/04/2554]

30. Launder, B. E. and D. B. Spalding, 1972, **Mathematical Models of Turbulence**, Academic Press.

31. Lee, A., Lewis, D. and Ashman, P., 2010, "Energy requirements and economic analysis of a full-scale microbial flocculation system for microalgal harvesting", **Chemical Engineering research and design**, 88: 988–996.

32. EngineeringToolbox. **Equivalent Diameter** [Online], Available: http://www.engineeringtoolbox.com/equivalent-diameter-d_205.html [20/04/2011].

33. Haizhijiao, Q. **Spirulina Platensis and Maxima** [Online], Available: http://biotech-health.en.made-in-china.com/product/xMDQyKJdCoRe/China-Spirulina-Platensis-and-Maxima.html [20/03/2011].

34. FAO. **Algal production** [Online], Available: http://www.fao.org/docrep/003/w3732e/w3732e06.htm [20/04/2011].

35. Kunjapur, A.M. and R.B. Eldridge, 2010, "Photobioreactor design for commercial biofuel production from microalgae**", Ind. Eng. Chem. Res.** ***Industrial and Engineering Chemistry Research***, 2010. 49(8): p. 3516-3526.

36. Wu, X. and J.C. Merchuk, 2002, "Simulation of algae growth in a bench-scale bubble column reactor", **Biotechnology and bioengineering**, 80(2): p. 156-168.

37. Hickin, E. J., 2003, Meandering Channels. In: Middleton, Gerard V., **Encyclopedia of Sediments and Sedimentary Rocks**, New York: Springer, pp. 432.

38. Power Plant CCS, **Raceway ponds** [Online], Available: http://www.powerplantccs.com/ccs/cap/fut/alg/raceway_ponds.html [20/07/2011].

APPENDIX A

Calculation of Reynold's Number in Open Channel Flow and Volume fraction of Algae cells

A.1 Reynold's Number calculation for open channel

For open channels, hydraulic radius, R_h (m), can be calculated by the following expression [23];

$$R_h = \frac{dw_c}{2d + w_c}$$

Where w_c is the channel width (m), d is the channel depth (m). Thus,

$$R_h = \frac{0.3 \times 3.95}{(2 \times 0.3) + 3.95} = 0.260$$

For open channels, a Reynold's number ($Re_{channel}$) of over 4,000 indicates turbulent flow, in this case,

$$Re_{channel} = \frac{\rho v R_h}{\mu}$$

This research defined velocity at least 0.1 m·s^{-1}.

$$Re_{channel} = \frac{1030 \times 0.1 \times 0.260}{1.31 \times 10^{-3}} = 2.044 \times 10^4$$

Thus the flow at velocity of 0.1 m·s^{-1} is turbulence and it is sufficient to suspend the algal cells.

A.2 Conversing volume fraction of algae from its concentration

This research defined concentration of algae dry cell at 1200 mg/L. However, algae was assumed to be *Spirulina platensis* species. Thus,

$$Volume\ fraction = 1200 \frac{mg}{L_{total}} \times \frac{1}{1300} \frac{m^3_{algae}}{kg} \times \frac{1000\, L_{algae}}{1 m^3_{algae}} \times \frac{1 kg}{10^6\, mg}$$

$$= 0.000923 \frac{L_{algae}}{L_{total}}$$

Volume fraction of 0.000923 was rounded up to 0.001 in this study.

APPENDIX B

The Specification of Domains and Boundary Conditions

B.1 New materials creating

Table B.1 Seawater creating

Tab	Setting	Value
Material Properties	Option	General Material
	Thermodynamic Properties > equation of state > Molar Mass	18.02 [kg kmol^-1]
	Thermodynamic Properties > equation of state > Density	1030 [kg m^-3]
	Transport Properties > Dynamic Viscosity	(Select)
	Transport Properties > Dynamic Viscosity > Dynamic Viscosity	0.00131 [Pa S]

Table B.2 Algae creating

Tab	Setting	Value
Material Properties	Option	General Material
	Thermodynamic Properties > equation of state > Molar Mass	588.69 [kg kmol^-1]
	Thermodynamic Properties > equation of state > Density	1300 [kg m^-3]
	Transport Properties > Dynamic Viscosity	(Select)
	Transport Properties > Dynamic Viscosity > Dynamic Viscosity	0.0042 [Pa S]

B.2 Analysis type Setting

Table B.3 Analysis type Setting

Tab	Setting	Value
Basic Setting	Analysis Type > Option	Steady State

B.3 Domains and boundaries creating

B. 3.1 Paddle wheel domain

Table B.4 Paddle wheel domain creating

Tab	Setting	Value
	Location and Type > Location	Paddlewheel
Basic Setting	Location and Type > Domain Type	Immersed Solid
	Domain Models > Domain Motion > Option	Rotating
	Domain Models > Domain Motion > Angular Velocity	35 [rev min^-1]
	Domain Models > Domain Motion > Axis Definition > Option	Two Points
	Domain Models > Domain Motion > Axis Definition > Rotation Axis From (X, Y, Z)	(0, 0.77, 0)
	Domain Models > Domain Motion > Axis Definition > Rotation Axis To (X, Y, Z)	(4, 0.77, 0)

B. 3.2 Raceway Domain

B.3.2.1 Body: Raceway1

Table B.5 Raceway1 body creating

Tab	Setting	Value
Basic Setting	Location and Type > Location	Raceway1
	Location and Type > Domain Type	Fluid Domain
	Fluid and Particle Definition > algae > Option	Material Library
	Fluid and Particle Definition > algae > Material	Algae
	Fluid and Particle Definition > algae > Morphology > Option	Dispersed Solid
	Fluid and Particle Definition > algae > Morphology > Mean Diameter	47.7 [micron]
	Domain Models > Pressure > Reference Pressure	1 [atm]
	Domain Models > Buoyancy > Option	Buoyant
	Domain Models > Buoyancy > Gravity X Dirn.	0 [m s^-2]
	Domain Models > Buoyancy > Gravity Y Dirn.	-g
	Domain Models > Buoyancy > Gravity Z Dirn.	0 [m s^-2]
	Domain Models > Buoyancy > Buoy. Ref. Density	1030 [kg m^-3]
	Domain Models > Buoyancy > Ref. Location > Option	Automatic
Fluid Models	Turbulence > Option	Fluid Dependent
Fluid Specific Models	algae > Fluid Buoyancy Model	Density Difference
	algae > Turbulence > Option	Dispersed Phase Zero Equation
	seawater > Fluid Buoyancy Model	Density Difference
	Seawater > Turbulence > Option	k-Epsilon
Fluid Pair Models	algae | seawater > Interphase Transfer > Option	Particle Model
	algae | seawater > Momentum Transfer > Drag Force > Option	Schiller Naumann

Table B.6 Top-slip wall boundary condition of Raceway1

Tab	Setting	Value
Basic Setting	Boundary Type	Wall
	Location	Raceway1Top
Boundary Details	Mass and Momentum > Option	Free Slip Wall
	Wall Contract Model	Use Volume Fraction

Table B.7 Default boundary of Raceway1

Tab	Setting	Value
Basic Setting	Boundary Type	Wall
	Location	Raceway1Default
Boundary Details	Mass and Momentum > Option	Free Slip Wall
	Wall Roughness	Smooth Wall
	Wall Contract Model	Use Volume Fraction

B.3.2.2 Body: Raceway2

Table B.8 Raceway2 body creating

Tab	Setting	Value
Basic Setting	Location and Type > Location	Raceway2
	Location and Type > Domain Type	Fluid Domain
	Fluid and Particle Definition > algae > Option	Material Library
	Fluid and Particle Definition > algae > Material	Algae
	Fluid and Particle Definition > algae > Morphology > Option	Dispersed Solid
	Fluid and Particle Definition > algae > Morphology > Mean Diameter	47.7 [micron]
	Domain Models > Pressure > Reference Pressure	1 [atm]
	Domain Models > Buoyancy > Option	Buoyant
	Domain Models > Buoyancy > Gravity X Dirn.	0 [m s^-2]
	Domain Models > Buoyancy > Gravity Y Dirn.	-g
	Domain Models > Buoyancy > Gravity Z Dirn.	0 [m s^-2]
	Domain Models > Buoyancy > Buoy. Ref. Density	1030 [kg m^-3]
	Domain Models > Buoyancy > Ref. Location > Option	Automatic
Fluid Models	Turbulence > Option	Fluid Dependent
Fluid Specific Models	algae > Fluid Buoyancy Model	Density Difference
	algae > Turbulence > Option	Dispersed Phase Zero Equation
	seawater > Fluid Buoyancy Model	Density Difference
	Seawater > Turbulence > Option	k-Epsilon
Fluid Pair Models	algae | seawater > Interphase Transfer > Option	Particle Model
	algae | seawater > Momentum Transfer > Drag Force > Option	Schiller Naumann

Table B.9 Top-slip wall boundary condition of Raceway2

Tab	Setting	Value
Basic Setting	Boundary Type	Wall
	Location	Raceway2Top
Boundary Details	Mass and Momentum > Option	Free Slip Wall
	Wall Contract Model	Use Volume Fraction

Table B.10 Default boundary of Raceway2

Tab	Setting	Value
Basic Setting	Boundary Type	Wall
	Location	Raceway2Default
Boundary Details	Mass and Momentum > Option	Free Slip Wall
	Wall Roughness	Smooth Wall
	Wall Contract Model	Use Volume Fraction

B.3.2.3 Body: Bend1

Table B.11 Bend1 body creating

Tab	Setting	Value
Basic Setting	Location and Type > Location	Bend1
	Location and Type > Domain Type	Fluid Domain
	Fluid and Particle Definition > algae > Option	Material Library
	Fluid and Particle Definition > algae > Material	Algae
	Fluid and Particle Definition > algae > Morphology > Option	Dispersed Solid
	Fluid and Particle Definition > algae > Morphology > Mean Diameter	47.7 [micron]
	Domain Models > Pressure > Reference Pressure	1 [atm]
	Domain Models > Buoyancy > Option	Buoyant
	Domain Models > Buoyancy > Gravity X Dirn.	0 [m s^-2]
	Domain Models > Buoyancy > Gravity Y Dirn.	-g
	Domain Models > Buoyancy > Gravity Z Dirn.	0 [m s^-2]
	Domain Models > Buoyancy > Buoy. Ref. Density	1030 [kg m^-3]
	Domain Models > Buoyancy > Ref. Location > Option	Automatic
Fluid Models	Turbulence > Option	Fluid Dependent
Fluid Specific Models	algae > Fluid Buoyancy Model	Density Difference
	algae > Turbulence > Option	Dispersed Phase Zero Equation
	seawater > Fluid Buoyancy Model	Density Difference
	Seawater > Turbulence > Option	k-Epsilon
Fluid Pair Models	algae | seawater > Interphase Transfer > Option	Particle Model
	algae | seawater > Momentum Transfer > Drag Force > Option	Schiller Naumann

Table B.12 Top-slip wall boundary condition of Bend1

Tab	Setting	Value
Basic Setting	Boundary Type	Wall
	Location	Bend1Top
Boundary Details	Mass and Momentum > Option	Free Slip Wall
	Wall Contract Model	Use Volume Fraction

Table B.13 Default boundary of Bend1

Tab	Setting	Value
Basic Setting	Boundary Type	Wall
	Location	Bend1Default
Boundary Details	Mass and Momentum > Option	Free Slip Wall
	Wall Roughness	Smooth Wall
	Wall Contract Model	Use Volume Fraction

B.3.2.4 Body: Bend2

Table B.14 Bend1 body creating

Tab	Setting	Value
Basic Setting	Location and Type > Location	Bend2
	Location and Type > Domain Type	Fluid Domain
	Fluid and Particle Definition > algae > Option	Material Library
	Fluid and Particle Definition > algae > Material	Algae
	Fluid and Particle Definition > algae > Morphology > Option	Dispersed Solid
	Fluid and Particle Definition > algae > Morphology > Mean Diameter	47.7 [micron]
	Domain Models > Pressure > Reference Pressure	1 [atm]
	Domain Models > Buoyancy > Option	Buoyant
	Domain Models > Buoyancy > Gravity X Dirn.	0 [m s^-2]
	Domain Models > Buoyancy > Gravity Y Dirn.	-g
	Domain Models > Buoyancy > Gravity Z Dirn.	0 [m s^-2]
	Domain Models > Buoyancy > Buoy. Ref. Density	1030 [kg m^-3]
	Domain Models > Buoyancy > Ref. Location > Option	Automatic
Fluid Models	Turbulence > Option	Fluid Dependent
Fluid Specific Models	algae > Fluid Buoyancy Model	Density Difference
	algae > Turbulence > Option	Dispersed Phase Zero Equation
	seawater > Fluid Buoyancy Model	Density Difference
	Seawater > Turbulence > Option	k-Epsilon
Fluid Pair Models	algae | seawater > Interphase Transfer > Option	Particle Model
	algae | seawater > Momentum Transfer > Drag Force > Option	Schiller Naumann

Table B.15 Top-slip wall boundary condition of Bend2

Tab	Setting	Value
Basic Setting	Boundary Type	Wall
	Location	Bend2Top
Boundary Details	Mass and Momentum > Option	Free Slip Wall
	Wall Contract Model	Use Volume Fraction

Table B.16 Default boundary of Bend2

Tab	Setting	Value
Basic Setting	Boundary Type	Wall
	Location	Bend2Default
Boundary Details	Mass and Momentum > Option	Free Slip Wall
	Wall Roughness	Smooth Wall
	Wall Contract Model	Use Volume Fraction

B.4 Interphases Boundary Setting

B.4.1 Raceway1-Bend1

Table B.17 Interphases boundary setting of Raceway1-Bend1

Tab	Setting	Value
Basic Setting	Interface Type	Fluid Fluid
	Interface Side 1 > Domain (Filter)	Raceway1
	Interface Side 1 > Region List	ToBend1
	Interface Side 2 > Domain (Filter)	Bend1
	Interface Side 2 > Region List	ToRaceway1
	Interface Models > Option	General Connection

B.4.2 Bend1-Raceway2

Table B.18 Interphases boundary setting of Bend1-Raceway2

Tab	Setting	Value
Basic Setting	Interface Type	Fluid Fluid
	Interface Side 1 > Domain (Filter)	Bend1
	Interface Side 1 > Region List	To Raceway2
	Interface Side 2 > Domain (Filter)	Raceway2
	Interface Side 2 > Region List	ToBend1
	Interface Models > Option	General Connection

B.4.3 Raceway2-Bend2

Table B.19 Interphases boundary setting of Raceway2-Bend2

Tab	Setting	Value
Basic Setting	Interface Type	Fluid Fluid
	Interface Side 1 > Domain (Filter)	Raceway2
	Interface Side 1 > Region List	ToBend2
	Interface Side 2 > Domain (Filter)	Bend2
	Interface Side 2 > Region List	ToRaceway2
	Interface Models > Option	General Connection

B.4.4 Bend1-Raceway1

Table B.20 Interphases boundary setting of Bend1-Raceway1

Tab	Setting	Value
Basic Setting	Interface Type	Fluid Fluid
	Interface Side 1 > Domain (Filter)	Bend2
	Interface Side 1 > Region List	To Raceway1
	Interface Side 2 > Domain (Filter)	Raceway1
	Interface Side 2 > Region List	ToBend2
	Interface Models > Option	General Connection

B.5 Global Initialization Setting

Table B.21 Global initialization setting

Tab	Setting	Value
Fluid Settings	Fluid Specific Initialization > algae > Initial Conditions > Velocity Type	Cartesian
	Fluid Specific Initialization > algae > Cartesian Velocity Components > Option	Automatic with Value
	Fluid Specific Initialization > algae > Cartesian Velocity Components > U	0 [m s^-1]
	Fluid Specific Initialization > algae > Cartesian Velocity Components > V	0 [m s^-1]
	Fluid Specific Initialization > algae > Cartesian Velocity Components > W	0 [m s^-1]
	Fluid Specific Initialization > algae > Volume Fraction > Option	Automatic with Value
	Fluid Specific Initialization > algae > Volume Fraction > Volume Fraction	0.001
	Fluid Specific Initialization > seawater > Initial Conditions > Velocity Type	Cartesian
	Fluid Specific Initialization > seawater > Cartesian Velocity Components > Option	Automatic with Value
	Fluid Specific Initialization > seawater > Cartesian Velocity Components > U	0 [m s^-1]
	Fluid Specific Initialization > seawater > Cartesian Velocity Components > V	0 [m s^-1]
	Fluid Specific Initialization > seawater > Cartesian Velocity Components > W	0 [m s^-1]
	Fluid Specific Initialization > seawater > Volume Fraction > Option	Automatic with Value
	Fluid Specific Initialization > seawater > Volume Fraction > Volume Fraction	0.999

B.6 Solver Control Setting

Table B.22 Solver control setting

Tab	Setting	Value
Basic Setting	Advection Scheme > Option	Upwind
	Turbulence Numerics	First Order
	Convergence Control > Max. Iterations	2000
	Fluid Timescale Control > Timescale Control	Auto Timescale
	Fluid Timescale Control > Length Scale Option	Conservative
	Fluid Timescale Control > Time Scale Factor	1.0
	Convergence Criteria > Residual Type	RMS
	Convergence Criteria > Residual Target	1E-04

APPENDIX C

Calculation of Power Required for Mixing by Paddle Wheel

C.1 Calculation of power required for mixing by a paddle wheel

The required power needed for mixing can be provided either by the mechanical or through hydraulic means. The force dissipated by a paddle can be determined as follows:

$$F_P = \frac{C_D A_p v_P^2}{2}$$

The drag coefficient, C_D, is a function of the paddle dimentions and flow conditions (Reynolds number). The commonly used value for C_D is 1.8. This research defined the paddle area which submerged in seawater is about 1.173 m^2 while the relative velocity of the paddle with respect to the water can be found from the simulation result in CFD-Post. The standard model with 37 rpm of the paddle wheel operation is the example case for this calculation. Thus,

$$F_P = \frac{1.8 \times 1030 \frac{kg}{m^3} \times 1.173 m^2 \times (0.867 \frac{m}{s})^2}{2} = 817.318 \text{ N}$$

Considering a 0.75 m diameter of a paddle wheel, the force of the water against the paddle is approximately 817.318 N. Thus the torque would be following

$$\tau = F_P \times r = 817.318 \times 0.75 = 612.988 \text{ N m}$$

Multiplying by 8 to find the torque required by all of impeller blades gives a required torque of approximately 4903.9 N m. The power requirement is simply the required torque multiplied by the rotational speed (37 rpm = 11.624 rad/s):

$$P = 4903.9 \text{ N m} \times 11.624 \frac{rad}{s} = 19001 \text{ W} = 19.001 \text{ kW}$$

Therefore, the 37 rpm of the paddle wheel operation in the standard raceway pond required mixing energy of 19.001 kW.

CURRICULUM VITAE

NAME Miss Kawisra Sompech

DATE OF BIRTH 25 March 1987

EDUCATIONAL RECORD

HIGH SCHOOL	High School Graduation Chiang Mai University Demonstration School, 2006
BACHELOR'S DEGREE	Bachelor of Science (Industrial Chemistry) Chiang Mai University, 2009
MASTER'S DEGREE	Master of Engineering (Chemical Engineering) King Mongkut's University of Technology Thonburi, 2011